Establishment of THP-1 Monocytes with Compromised Mitochondrial Functions.

A thesis

submitted in partial fulfilment

of the requirements for the degree

of

Master of Science in Biological Sciences

at

The University of Waikato

by

Tzu-wen Joy Chou

THE UNIVERSITY OF
WAIKATO
Te Whare Wānanga o Waikato

The University of Waikato

2009

ABSTRACT

The process of inflammation is important for both normal health and in a number of diseases, such as metabolic disorders, autoimmune diseases, and neurodegenerative diseases. Mitochondria are vital for the functioning of all cells. It had been implicated as a key player in inflammatory processes, especially through reactive oxygen species as signals of various immune responses. This study aimed to establish a THP-1 cell line with compromised mitochondrial functions, using antimycin A as a Complex III inhibitor, and to investigate the role of mitochondrial stress, as monitored by the expression of Hsp60, in inflammatory processes.

High concentrations of antimycin A (100 and 200 μM) were cytotoxic to THP-1 monocytes that they were rapidly killed within 48 hours of exposure. Lower concentrations of antimycin A (5, 10, 25 and 50 μM) gave growth inhibition effects to THP-1 monocytes. Pyruvate and uridine were used with an intention of rescuing the THP-1 cell growth at lower antimycin A concentrations. The THP-1 monocytes treated with antimycin A with uridine and pyruvate showed more growth compared to the ones without uridine and pyruvate supplement. Yet this difference is insignificant statistically. The expressions of Hsp60 and TNF-α at the mRNA level was monitored using reverse transcriptase polymerase chain reaction. Hsp60 expression from THP-1 monocytes only showed some minor fluctuations in different antimycin A concentrations, regardless of uridine and

pyruvate supplement, indicating the stress mitochondrial response was unobvious. On the other hand, TNF-α expression was dramatically down-regulated in THP-1 monocytes treated with antimycin A only compared to the untreated control and ones supplemented with uridine and pyruvate. These results suggest that antimycin A may have inhibition effect towards TNF-α expression, and uridine and pyruvate could also have other functions in THP-1 monocytes apart from redox rescue compounds. Yet the mitochondrial stress response shown by Hsp60 induction still remains to be further investigated.

ACKNOWLEDGEMENT

First of all, I would like to sincerely thank Dr. Ryan Martinus, my supervisor, for his expertise and time, including personal, to coach me through this project. Also to Julie Goldsbury, our Laboratory Manager, thank you for supplying the materials and resources, as well as helping me with problems during the experimental procedures. And to An-chi and Bei, thank you for sharing your experiences and understanding with me. You saved me a lot of time figuring out protocols.

For the people from other laboratories, I am much appreciated with Kerry Allen, the Laboratory Manager of Honey Research Unit, who looked after our daily procedures when Julie was away. And Sam, thank you for writing the source code for my statistical analysis on R, as well as being my personal "Computer Support Trouble Shooter". None of these would happen without you. Another big thank you to Dr. Ray Cursons, Professor Dick Wilkons, thank you for your expert opinions provided when I ran into problem during my experiments while I working alone. Also to the rest of people from Honey Research Unit and Molecular Genetics Research, thank you for your friendship and being our "back-up stores", allowing us to borrow things from you, when we happened to run out.

To the general staff in the University, thank you Cheryl, our Science Librarian, for helping me with all the formatting and EndNote editing for my thesis. Thank you Jonathan, for guiding me through the experimental procedures at the beginning of my work. And to other staff of the University who gave mental support to my studying, thank you all.

I cannot say how much appreciated I am with my family. You fully stood on my side through the entire process and experienced all the highs and lows with me. Thank you for your unconditional care. Last but not least, thank you all my friends who cheered me up when I was disappointed and celebrated with me for my success.

TABLE OF CONTENT

LIST OF FIGURES

LIST OF TABLES

LIST OF ABBREVIATIONS

3-(N-morpholino) propanesulfonic acid = MOPS

Activator Protein-1 = AP-1

Antimycin A = AA

Diethylpyrocarbonate = DEPC

Dithiothreitol = DTT

Electron transport system = ETS

Enzyme-linked immunosorbent assay = ELISA

Ethylenediaminetetraacetic acid = EDTA

Extracellular signal-regulated kinase = ERK

Glyceraldehyde 3-phosphate dehydrogenase = GAPDH

Heat shock protein = Hsp

Interleukin = IL

Janus-kinase = JNK

Mitogen activated kinase = MAPK

Nuclear factor-κB = NF-κB

Reverse transcriptase = RT

Sodium borate = SB

Toll-like receptor = TLR

Tris-EDTA = TE

Tumor necrosis factor-α = TNF-α

Type 1 or 2 Diabetes Mellitus = T1DM or T2DM

Uncoupling protein = UCP

Uridine and pyruvate supplement = UP

CHAPTER ONE

LITERATURE REVIEW

1.1 Inflammatory Response

Inflammation response is broadly specific, induced by infection or cell damage. It also responds to cytokines released by cells of adaptive immune response. The classic signs of inflammation are vasodilation (redness and heat), swelling and pain. Vasodilation is caused by increased diameter of local blood vessels, allowing increased blood flow to affected areas. Swelling is because of increased adhesion of leukocytes to local blood vessel walls and enhanced capillary permeability, encouraging influx of leukocytes. The pain is due to both swelling and the stimulation of pain receptor in skin mediated by peptide bradykinin (Mak & Saunders, 2006).

Damaged tissue or cells release chemotactic molecules such as C5a, attracting macrophages and neutrophils, the main leukocytes involved in inflammation. These leukocytes push through blood vessels entering damaged sites. The concentration gradients of chemotactic molecules (i.e. chemotaxis) are required for subsequent cell migration.

The initiation of inflammation is not well understood. It is possibly triggered by proteins released from damaged tissue due to infection or injury. Mediators like proinflammatory cytokines, TNF-α and IL-6 are secreted by macrophages to activate down-stream inflammatory responses. TNF-α and IL-6 are sent by activated macrophages to hepatocytes in the liver, which respond with the systematic production of acute-phase proteins. These proteins bind to a wide range of bacterial agents, thereby eliminating pathogens or "antigens" in a less specific way.

A number of innate immune cells have pattern recognition molecules on their cell surfaces as binding receptors of antigens. Series of signal transduction pathways can be activated after antigens bind to these receptors. Examples of these pattern recognition molecules on the cell surfaces of monocytes and macrophages include cluster of differentiation 14 (CD14), toll-like receptors 2 and -4 (TLR2 and TLR4). The signal cascades then stimulate other nuclear transcription factors for more inflammatory responses or stimulating adaptive immune responses. Inflammation is therefore an important bridge between innate and adaptive immune responses (Mak &Saunders, 2006).

Impaired inflammation is related to deleterious consequences of many pathologies, including neurodegeneration to central nervous system such as Alzheimer's disease, Parkinson's disease and multiple sclerosis (Centonze *et al.,* 2007; Esiri,

2007), and autoimmune diseases due to antigen from one's own body. Some examples of autoimmune diseases likely to be associated with inflammation are Type One Diabetes Mellitus (T1DM), Kawasaki's disease, Sjorgen's disease and rheumatoid arthritis.

1.2 Mitochondria and Oxidative Phosphorylation

Mitochondria are sites of oxidative phosphorylation, citric acid cycle and β-oxidation of free fatty acids (Bailey *et al*., 2005). ROS are produced in Complex I (NADH / ubiquinone oxidoreductase) and III (ubiquinol / cytochrome *c* oxido-reductase) of electron transport system (ETS) (Fleury *et al*., 2002). The major ROS generated, superoxide anion (O_2^-), hydrogen peroxide (H_2O_2) and hydroxyl radical ($OH^{\cdot}$), are by-products from ETS and are also stimuli for apoptosis (Fleury *et al*., 2002). O_2 is converted to O_2^- because of a single electron leakage from one of the mitochondrial complexes. O_2^- is then converted into H_2O_2 with the catalysing effect of superoxide dismutase. H_2O_2 is further changed into $OH^{\cdot}$ in presence of Fe^{2+}. Despite these ROS produced during oxidative phosphorylation, natural antioxidants such as superoxide dismutase, glutathione reductase and glutathione peroxidase are present in mitochondria (Fleury *et al*., 2002). Another important mitochondrial protein associated with increased ROS production is uncoupling protein-2 (UCP2). UCP2 diminishes mitochondrial ROS production by lowering the mitochondrial membrane potential (Arsenijevic *et al*., 2000), and is up-regulated in response to increased ROS in macrophages (Giardina *et al*.,

2008). In some circumstances however, ROS generated overwhelm the protection effect of antioxidants. This phenomenon is termed oxidative stress.

Mitochondrial oxidative stress is known as an important factor in ageing, which can induce intrinsic apoptosis to drive tissue ageing (Sastre *et al*., 2003). ROS have the potential to damage proteins, lipids and DNA (Halliwell, 1992, 2001). Oxidative stress-mediated mitochondrial impairment and/or dysfunction are increasingly believed to play key roles in many diseases including arthritis (Vaille *et al*., 1990), ischemic diseases (Omar & McCord, 1991), Alzheimer's disease, Parkinson's disease (Mattson & Kroemer, 2003; Reddy & Beal, 2005), and many others.

1.2.1 Role of ROS in the Immune System

Yet apart from causing damages, ROS is also adapted by the immune system in higher organisms as defense mechanisms and to initiate further responses. Neutrophils and macrophages produce superoxide radical with NADPH oxidase to fight with invading pathogens (McCord, 2000). In addition, superoxide is a mediator of inflammation. Superoxide and hydrogen peroxide can activate kinase signaling cascades, including protein kinase C (Klann *et al*., 1998), mitogen-activated protein kinase (MAPK) and transcription factors (Droge, 2002). Chronic oxidative stress subsequently causes the activation of transcription factors, NF-κB and AP-1, followed by the induction of other genes producing pro-inflammatory

cytokines, such as tumor necrosis factor-α (TNF-α), interleukin-1 and -6 (IL-1 and IL-6) and other downstream inflammatory responses (Tse *et al*., 2004). Inflammation is increasingly being recognised as a cause of major metabolic and neurodegenerative diseases, including Type 2 Diabetes (T2D), atherosclerosis, Alzheimer's Disease, Parkinson's Disease and dementia (Bozner *et al.*, 2002; Tytell & Hooper, 2001). Since ROS are critical to the immune system and many aetiologies, catalytic antioxidants were seen as a potential drug target for inflammatory diseases. Catalytic antioxidants applied to lipopolysaccharide-induced macrophages suppressed proinflammatory cytokine and ROS production via inhibition of NF-κB DNA binding, without affecting MAPK signalling pathway. Catalytic antioxidants were thus claimed by the authors as protection in chronic inflammatory diseases (Tse *et al*., 2004).

1.3 Stress Proteins – The Counteracting Molecules in Mitochondria for Cellular Stress

An early counteracting activity of oxidative stress inside mitochondria is the up-regulation of heat shock proteins (Hsps) or chaperones, a class of mitochondrial stress protein that is one of the members of heat shock protein family, to protect other macromolecules. Hsps were discovered by Ferrucio Ritossa and co-workers in 1962: heat shock induced puffing patterns in the polytene chromosomes of salivary glands in *Drosophila melanogaster* larva (Ritossa, 1962). Hsp genes were latter identified in 1974 so introduced the term "heat shock proteins" (Tissieres *et*

al., 1974). Hsp gene sequences are highly conserved and present in prokaryotes and eukaryotes (Pockley, 2003), which are named based on molecular weights. The Hsp that this study focused on is Hsp60 with its molecular weight as 60kDa. Hsp60 is the eukaryotic homologue of bacterial GroEL protein, which is located in the matrix of mitochondria (Randord *et al*., 2000). Hsp10 is the co-chaperone of Hsp60. These two Hsps form a complex that function in co-operation. In eukaryotes, the protein is encoded in the nuclear DNA, synthesised in the cyctosol then imported into the mitochondria. It assists proper folding of newly synthesised polypeptides, facilitating protein transport through membrane channels, preventing aggregation and denaturation of proteins under heat shock, as well as refolding the denatured proteins back into their naïve structures (Hartl, 1996). Hsp60 is thus vital for maintaining cellular homeostasis and tolerance to stresses.

Moreover, hsp60, Hsp70 and Hsp90, both alone and in combination, protect against intracellular β-amyloid stress. The Complex IV inhibition effect of β-amyloid was neutralised by Hsp60 (Veereshwarayya *et al*., 2006). Plus Hsp60 and Hsp10 in combination or individually protect mitochondrial integrity and oxidative phosphorylation capacity during ischemia/reperfusion injury in cardiac myocytes (Lin *et al*., 2001).

1.3.1 Role of Hsp60 in the Immune Response

It was thought that eukaryotic Hsp60 is only located in the mitochondria, however, recent evidence indicate that this protein is expressed on the plasma membranes of cells and indeed secreted from cells under stress conditions (Maguire *et al*., 2002a). Immunoprecipitation studies showed that hsp60 is also located on the cell surface (Gupta & Austin, 1987). Apart from its chaperonin function, Hsp60 is also antiapoptotic by forming macromolecular complexes with bak and bax to block the release of cytochrome *c* and the subsequent caspase (Kirchhoff *et al*., 2002).

The role of Hsp60 played in immune response was not realised until Hsp60 was discovered to have a dual function of chaperonin and signalling (Maguire *et al*., 2002b). Extracellular, bacterial hsp60 are detected by the receptor on macrophages. The detection then activated the signalling pathway to nucleus, switching on transcription factor NF-κB, thereby producing inflammatory cytokines such as TNF-α, IL-1β, IL-6, and IL-8 (Lewthwaite *et al*., 2007). Also bacterial Hsp60 was discovered to act as an antigen to T-cells, despite their sequence homology to human Hsp60 (Schwartz & Cohen, 2000). Many studies confirmed that both human and bacterial Hsp60, if present at the cell surface of immune cells, are links between innate and adaptive immune responses. When detected by the cell surface receptors such as CD14, TLR-2 and TLR-4, they are seen as antigens by human monocytes, macrophages and dendritic cells, as well as ligands for antigen receptors in T-cells and B-cells ((Zhao *et al*., 2007), reviewed in (Praeres da Costa *et al.*, 2003; Zhao *et al.*, 2007)). The follow-on effect of this

is the activation of serine/threonine kinase cascade involving mitogen-activated protein kinases (MAPK), p38, janus-kinase (JNK) and extracellular signal-regulated kinases (ERK), switching on the transcription factors AP-1 and NF-κB in the nucleus, thereby producing pro-inflammatory cytokines and other inflammatory responses (Lewthwaite *et al*., 2007; Wallin *et al*., 2002; Zanin-Zhorov *et al*., 2005). Mammalian Hsp60 acts as a target antigen in Type 1 Diabetic (T1D) mice (Elias *et al*., 1991). Hsp60 is therefore a danger signal in the immune system (Chen *et al*., 1999).

The signaling pathways of extracellular Hsps (cpn60, -70 and gp 96) in monocytes, macrophages and dendritic cells had been elucidated as many studies focused on adding extracellular Hsp60 to immune cells and observing the effects. However, relatively little had been done on the secretion of Hsp60 from the mitochondria. Two recent studies had shown that the intracellular secretion of Hsp60 and -70 in cardiac muscles are likely to be via attaching to the membrane of exosomes, a type of intracellular vesicle likely to contain lipid rafts (Lancaster & Febbraio, 2005; Gupta & Knowlton, 2007). Yet no such work had been done on monocytes and macrophages or the effect of intracellular Hsp60 on the MAPK cascade due to mitochondrial dysfunction in these cells.

1.4 Cell Culture Model Systems for Studying Mitochondrial Dysfunction

A special type of cell line called *rho zero* cells (ρ^o) are very useful to study follow-on consequences of compromised mitochondrial functions. ρ^o cells have their mitochondrial DNA depleted by a mitochondrial DNA inhibitor, usually ethidium bromide (Nagley *et al*., 1977). This means that their oxidative phosphorylation is dysfunctioned, so they rely on extensive glycolysis to generate cellular energy in the form of ATP. Many kinds of eukaryotic cells have been generated to become ρ^o. Examples include human Namalwa cells, a human B-type lymphoblastoid cell line (Larm *et al*., 1994; Martinus *et al*., 1993); HL-60, human promyelocytic leukemia cell line (Gómez-Díaz *et al*., 1997); rat hepatoma cells, H4 (Martinus *et al*., 1996) and human neuroblastoma cells, SH-SY5Y (Hyun *et al*., 2007). Alternatively cells with fully functioning mitochondria grown in prolonged anaerobic conditions can also be used to study mitochondrial dysfunction (Vaillant *et al*., 1991).

1.4.1 Maintenance of Cells Having Compromised Mitochondrial Functions

NAD^+ is converted to NADH during glycolysis. In normal oxidative phosphorylation, the resulting NADH is reoxidised to NAD^+. Yet this pathway will not provide adequate NAD^+ if the electron transport system (ETS) is partially or totally inavailable. Alternatively pyruvate can be converted to lactate as a route of NAD^+ production. For this reason extra pyruvate was added to cells relying

heavily on glycolysis for energy production (Guidarelli *et al.*, 2006; King & Attardi, 1989). Thus pyruvate can be called the "redox sink molecule" or "redox rescuer" for this kind of function.

Another pathway for ρº cells to generate enough NAD^+ is through the activity of plasma membrane redox system, consisting of a series of molecules transferring electrons from internal reductants such as NAD(P)H to external oxidants, thereby protecting cells against external oxidative stress (Alcain *et al*., 1991; del Castillo-Olivares *et al*., 2000). A key molecule in the plasma membrane redox system is Coenzyme Q_{10}, which protects lipids from oxidative stress in its reduced form. Coenzyme Q_{10} donates electrons to α-tocopherol radical and ascorbate free radical, therefore maintaining the reduced form of α-tocopherol and ascorbate that they can continuously scavenge free radicals (Kagan *et al*., 1990a, b). Indeed, Martinus *et al*., 1993 reported that ρº human Namalwa cells could be sustained by Coenzyme Q_{10} supplement. Martinus *et al*., 1993 also demonstrated that ferrycyanide, an anion impermeant to plasma membrane, could enhance ρº cell growth, possibly by acting as an extracellular electron acceptor, allowing the plasma membrane oxidase to reoxidise cytosolic NADH to NAD^+, thereby supplying more NAD^+ for glycolysis. Soon after then, it was discovered that the up-regulation of plasma membrane oxidoreductase activity is vital for human Namalwa ρº cells to survive. Inhibiting one of the enzymes from plasma membrane redox system, NADH-ferricyanide reductase with pCMBS caused rapid decease of the ρº cells (Larm *et al*., 1994).

Another blockage due to the malfunction of ETS is the pyrimidine biosynthetic pathway. The key enzyme involved in pyrimidine biosynthesis, dihydroorotate dehydrogenase complex, is coupled to the mitochondrial ETS (Jones, 1980). Uridine was therefore used to bypass this obstacle (Morais *et al*., 1980).

1.5 Types of Mitochondrial Inhibitors

Some examples of well-known mitochondrial inhibitors with their target and mode of actions are briefly summarised in this section, with a particular emphasis on antimycin A. Ethidium bromide is one of the intercalating agents with aromatic macrocycles composed of fused, heterocyclic rings, which inserts between DNA base pairs. The base pairs are forced apart to accommodate the intercalating agent. If too many inserted, it causes the double helix to unwind. Through this way ethidium bromide acts as a mitochondrial DNA inhibitor (Garret & Grisham, 2005). Rotenone, a mitochondrial Complex I inhibitor, prevents the electron transfer from iron-sulfur centres in Complex I to ubiquinone, the reaction catalysed by NADH-ubiquinone reductase. Oligomycin, an ATP Synthase inhibitor, binds to a subunit of F_0, and blocks the movement of protons through F_0 (Garret & Grisham, 2005).

Antimycin A was first identified by Leben and Keitt as a fungicide produced by *Streptomyces*, with its mitochondrial inhibitory effect firstly observed by Ahmad

and co-workers (Slater, 1973). Antimycin A is an electron transport Complex III inhibitor. It inhibits Coenzyme Q-cytochrome *c* reductase by blocking electron transfer between b_H and Coenzyme Q in the Q_n site (Garret & Grisham, 2005). It also causes a single electron leakage to oxygen that is supposed to go from the mobile head domain of Rieske iron-sulfur protein to cytochrome c_1 subunit (Nohl *et al*., 2003).

1.6 Use of Immune Cells in Cell Culture Model Systems

Model systems of human immune cell culture are useful to study complicated reactions of immune response, since one can do limited experimental assays with live humans due to human ethics. Cell lines that behave similarly compared to native cells in human body, together with the ability to differentiate into other immune cell types after chemical inductions, become preferential options for such model systems. In addition, it is even better if the chosen cell types are able to proliferate but not to self-differentiate into tissue cell types after certain number of cycles. Because human leukemia cell lines satisfy all the above conditions, they therefore are successful candidates of immune cell culture model systems. Examples of commonly used human leukemia cell lines include promyelocytic leukemia cell line HL-60 (Thompson *et al*., 1988) and acute leukemia monocyte THP-1 (Guidarelli *et al*., 2006; Zhuang *et al*., 1998). As HL60 can be induced into monocytes using 1α,25-dihydroxyvitamin D_3, (Mills *et al*., 1999) and THP-1 monocytes are able to differentiate into macrophages after the induction of phorbol myristic acetate (Auwerx, 1991), combined with their ability to produce

proinflammatory cytokines such as TNF-α, they are used extensively to study inflammatory and associated responses.

1.6 Outline of this Study

This study intended to establish a cell culture model system with compromised mitochondrial functions to study the relationship between inflammatory response and mitochondrial dysfunction. The experimental set-up is divided into four parts:

1. Establishing THP-1 monocytes with compromised mitochondrial functions using antimycin A;

2. Investigating the effect of redox rescue of antimycin A-treated monocytes with pyruvate and uridine to establish a long term culture of mitochondrial compromised cells;

3. Confirming the influence of mitochondrial stress by monitoring the expression of Hsp60 at the mRNA level;

4. Investigating the inflammatory response from THP-1 monocytes undergoing mitochondrial inhibition by monitoring the expression of TNF-α at the mRNA level.

CHAPTER TWO MATERIALS AND METHOD

2.1 Materials

2.1.1 Laboratory chemicals and reagents

All chemicals and reagents used in this project are listed in Table 1 together with their sources.

Table 1: Chemicals and reagents

Chemical or Reagent	Source
3-(N-morpholino) propanesulfonic acid (MOPS)	AppliChem
Agarose	AppliChem
Antimycin A	Sigma
Boric Acid	Ajax Finechem
Deionised formamide	Sigma
Diethyl pyricarbonate (DEPC)	Sigma
DNase treatment kit	Invitrogen
Ethidium bromide	Sigma
Ethylenediaminetetra-acetic acid (EDTA)	BDH Laboratory

	Supplies
Fetal bovine serum	Invitrogen
Gel loading dye	Ficoll
N-2-Hydroxyethylpiperazine-N-2-ethanesulphonic acid (HEPES)	BDH Laboratory Supplies
RPMI liquid growth medium	Invitrogen
RT-PCR kit	Invitrogen
Sodium acetate	Ajax Chemicals
Sodium pyruvate	Sigma
Streptomycin/penicillin	Ruakura Research Institute
Tris	AppliChem
TRIzol Reagent	Invitrogen
Uridine	Sigma

2.1.2 Stock Solutions

Stock solutions were routinely made in the laboratory. The compositions of these are listed in Table 2:

Table 2: Stock solutions

Solution	Composition
10X gel loading dye	0.75 g Ficoll, 6.25 mg Bromophenol blue, 0.5 mL 10X SB buffer, 4 mL sH_2O
10X MOPS buffer (pH 7)	83.7 g MOPS, 8.2 g sodium acetate, 2.9 g EDTA in 1 L sH_2O
10X SB buffer (pH 8.5)	28 g boric acid, 4.5 g sodium hydroxide in 1 L sH_2O
10X TBE buffer	108 g Tris, 55 g boric acid, 9.5 g EDTA in 1 L 0.01% DEPC water
Antimycin A	Powder in 95% ethanol (10 mM)
Ethanol	100% ethanol diluted with sH_2O (95%)
HEPES	Powder in sH_2O (0.25 mM)
Sodium pyruvate	Powder in sH_2O (100 mM)
Streptomycin/penicillin	Powder in sH_2O (5 mM)
TE buffer (pH 8.0)	10 mM Tris-HCl, 1 mM EDTA in 1 L 0.01% DEPC water
Uridine	Powder in sH_2O (20 mM)

2.1.3 Standard Growth Medium for THP-1 Cells

The liquid growth medium was routinely made in the laboratory containing the materials listed in Table 3:

Table 3: Components of THP-1 growth medium

Chemical or Reagent
0.25 mM HEPES
1 mM Sodium pyruvate
10% Fetal Bovaine Serum
1X RPMI liquid medium
50 μM Streptomycin/penicillin

The medium was filter sterilised with a 0.22 μM syringe filter (Sartorious Minisart®) and stored at 4°C, except being pre-incubated at 37°C for 30 min prior to use.

2.1.4 cDNA Synthesis with Reverse Transcriptase

The cDNA template was synthesised using components purchased from Roche.

Table 4: cDNA synthesis materials

Material Name	Content
Transciptor Reverse Transcriptase	25 U/μL
(Enzyme)	200 mM potassium phosphate
	2 mM dithiothreitol (DTT)
	0.2% (v/v) Triton X-100
	50% (v/v) Glycerol (pH 7.2)
5X RT Reaction Buffer	250 mM Tris-HCl
	150 mM KCl
	40 mM $MgCl_2$ (pH 8.5)
Protector RNase Inhibitor	40 U/μL
	20 mM HEPES-KOH
	50 mM KCl
	8 mM DTT
	50% glycerol (pH 7.6)
Anchored-Oligo(dT) 18 Primer	50 μM

Random Hexamer Primer	600 µM
Control RNA	50 ng/µL Stabilised solution with a total RNA fraction purified from K562 cell line
Control Primer Mix PBGD	5 µM forward and reverse primer Porphobilinogen deaminase (pH 8.3)
PCR Grade Water	Nuclease-free water

2.1.5 Polymerase Chain Reaction (PCR)

Polymerase chain reactions were performed with FastStart Taq Polymerase (Roche) and other materials purchased mostly from Roche.

Table 5: PCR Materials

Material Name	**Content**
FastStart Taq DNA Polymerase (Enzyme)	5 U/µL Storage buffer: 20 mM Tris-HCl (pH 9) 100 mM KCl

	0.1 mM EDTA
	1 mM DTT
	0.2% (v/v) Tween 20
	50% (v/v) Glycerol
10X PCR Reaction Buffer	500 mM Tris-HCl
with 20 mM $MgCl_2$ (pH 8.3)	100 mM KCl
	50 mM $(NH_4)_2SO_4$
DNA Ladder (Invitrogen)	10 mM Tris-HCl (pH 7.5)
	1 mM EDTA

The human GAPDH primer sequences were:

Forward: ACC ACA GTC CAT GCC ATC AC

Reverse: TCC ACC ACC CTG TTG CTG TA

Expected product size: 451 bp

The human Hsp60 primer sequences were:

Forward: TTC GAT GCA TTC CAG CT TG

Reverse: TTG GGC TTC CTG TCA CAG TT

Expected product size: 439 bp

The human TNF-α primer sequences were:

Forward: CAG AGG GAA GAG TTC CCC AG

Reverse: CCT TGG TCT GGT AGG AGA CG

Expected product size: 324 bp

2.2 Method

2.2.1 Cell Culture maintenance

The human acute monocytic leukaemia cell line, THP-1, was obtained from the University of Auckland. The cells were suspended in 10 cm^3 of the growth medium. The cultures were stored in a sterile flask with a filter cap (Nunclon^{TM} Δ Surface) and incubated in a sterile incubator at 37°C with 5% CO_2. The medium was changed every 10 days by centrifuging the cells at 389 rcf for 10 min (Heraeus Megafuge 1.0). After that the cells were re-suspended in the new growth medium. Cells were mixed with 0.4% tryphan blue stain (Sigma) in a 1:1 ratio, loaded on a haemocytometer then counted under a light microscope (Nikon Eclipse TS-100).

2.2.2 Mitochondrial Inhibition Assay

2.2.2.1 Mitochondrial Inhibition with Antimycin A

Antimycin A binds to the quinone reduction site of the cytochrome bc_1 complex, which is part of Complex III of the electron transport system (ETS) (Huang *et al.*, 2005; Reed *et al.*, 1978; Slater, 1973). Increase and leakage of superoxide radicals were also found in rat liver mitochondria treated with antimycin A (Piskemik *et al.*, 2008). Antimycin A is widely used as an inducer to study mitochondrial oxidative stress (Firth *et al.*, 2008; Zhuang *et al.*, 1998). In this experiment antimycin A was

dissolved in ethanol due to its insolubility in water. In a 24-well plate, 2 mL of assay mixtures were set up with the components listed in Table 6:

Table 6: Composition of cell culture models for mitochondrial inhibition assay

Chemical or Reagent	**Concentration**
THP-1 cell culture in RPMI medium	1.84×10^4 cells/mL
Antimycin A	5, 10, 25, 50, 100 or 200 μM respectively
Ethanol (solvent control)	Equivalent concentrations as antimycin A respectively
RPMI liquid medium	Make up to 2 mL

THP-1 cells grown in normal RPMI medium without any additives were used as untreated controls. Since antimycin A is soluble in ethanol, a growth study with equivalent concentrations (5, 10, 25, 50, 100 or 200 μM respectively) of ethanol without any mitochondrial inhibitors was carried out to determine the effect of ethanol towards THP-1 cell growth. These THP-1 cells grown in the presence of ethanol plus normal medium were used as solvent controls. All concentrations including the solvent and untreated controls were done in triplicates. The viable cell

numbers of all replicates were counted daily in a haemocytometer by tryphan blue stain exclusion. The media were changed on alternative days to avoid the accumulation of lactic acid. Pyruvate was converted to lactate to generate NAD^+ for glycolysis, when oxidative phosphorylation was impaired so could not re-generate enough NAD^+ from NADH. The average cell numbers and standard deviations for each antimycin A concentration were calculated based on the triplicates.

2.2.2.2 Mitochondrial Inhibition using Antimycin A, Supplemented with Uridine and Pyruvate

This experiment was repeated with 50 μg/mL uridine and 1 mM sodium pyruvate as pyrimidine biosynthesis intermediates and redox rescuers (or redox sink molecules), together with other components in 2 mL of assay mixtures. The media were also changed on alternative days to avoid accumulation of acidic waste products. The average cell numbers and standard deviations for each triplicate were calculated.

2.2.3 Antimycin A Dose-Response Assays for Assessing Hsp60 and TNF-α Expressions

2.2.3.1 Attempt One

In 24-well plates, 2 mL of assay mixtures were set up as shown in Table 4. The initial THP-1 cell concentration was 1.84×10^4 cells/mL. The final concentrations of

antimycin A were 5, 10, 25, 50, 100 and 200 μM respectively, with each concentration in triplicates. A separate set of the same concentrations (5, 10, 25, 50, 100 and 200 μM) of antimycin A were set up containing uridine and sodium pyuvate as descried in *2.2.2.2*. The final concentrations of uridine and sodium pyruvate were still 50 μg/mL and 1 mM respectively. The THP-1 cells were exposed to five days of different antimycin A concentrations, with media changed every 48 hours. The cells were pelleted on Day 4 at 2,000 × *g* for 7 min, and total RNA extracted (section 2.2.4.3) immediately after cell harvest.

2.2.3.2 Attempt Two

The same protocol as 2.2.3.1 was repeated. THP-1 cells were also treated with various antimycin A concentrations for five days. Yet the THP-1 cell concentration used this time was 1×10^5 cells/mL. The final antimycin A concentrations in wells were 5, 10, 25, 50 μM, plus an untreated control. The same antimycin A concentrations were used for uridine and sodium pyruvate treatment. An untreated control containing 50 μg/mL of uridine and 1 mM of sodium pytuvate was included. 100 and 200 μM of antimycin A were unnecessary since most of the THP-1 cells were killed within 48 hours under the exposure of such high concentrations of mitochondrial inhibitor, so not enough total RNA could be extracted.

2.2.4 TRIzol RNA Extraction

A series of trials for total RNA extraction and Reverse-Transcriptase Polymerase Chain Reactions (RT-PCR) were done to ensure that the reagents functioned properly and to optimise the protocols.

2.2.4.1 TRIzol RNA Extraction – Attempt One

1 mL of THP-1 cells (~2×10^5 cells/mL) was centrifuged (Centrifuge 5415 R, Eppendorf) at 13,000 rpm for 3 min. The cell pellets were resuspended in 500 µL TRIzol (Invitrogen) and incubated at 15-30°C for 5 min. 100 µL of chloroform was added, shaken vigorously by hand for 15 seconds and incubated at 15-30°C for 3 min. The mixture was centrifuged (Centrifuge 5415 R, Eppendorf) at 12,000 rpm for 15 minutes at 4°C. The upper colourless RNA layer was transferred to a new RNase-free tube. 250 µL of isopropanol was added to the RNA solution, incubated at 15-30°C for 10 min then centrifuged (Centrifuge 5415 R, Eppendorf) at 12,000 rpm for 10 min at 4°C. The RNA pellet was washed with 1 mL of 75% ethanol made with 0.01% DEPC (Sigma)-treated water, mixed well by vortex and centrifuged (Centrifuge 5415 R, Eppendorf) at 7,400 rpm for 5 min at 4°C. The supernatant was discarded. The RNA pellet was air dried on ice for 5-10 min. The pellet was resuspended in 30 µL of 1X TE buffer made with 0.01% DEPC-treated water (0.01 % DEPC water) (pH 8.0) and kept on ice. The purity of the extracted RNA was quantified with Nanodrop ND-1000 spectrophotometer. The remaining RNA sample was stored at −80°C.

2.2.4.2 TRIzol RNA Extraction – Attempt Two

500 µL of THP-1 cells (~2×10^5 cells/mL), instead of 1 mL, were centrifuged (Centrifuge 5415 R, Eppendorf) at 2000 × *g* for 7 min to maximise the TRIzol activity. The cell pellets were resuspend in 500 µL TRIzol and incubated at 15-30°C for 5 min. 100 µL of chloroform was added, shaken vigorously by hand for 15 sec and incubated at 15-30°C for 3 min. The mixture was centrifuged (Centrifuge 5415 R, Eppendorf) at 12,000 × *g* for 15 min at 4°C. The upper colourless RNA layer was transferred to a new RNase-free tube. 250 µL of isopropanol was added to precipitate the RNA. The content was incubated at 15-30°C for 10 min and at −20°C for 20 min. This was then centrifuged (Centrifuge 5415 R, Eppendorf) at 12,000 × *g* for 10 min at 4°C. The supernatant was removed. The RNA pellet was washed with 1 mL of 75% ethanol made with 0.01% DEPC water, mixed thoroughly by vortex and, centrifuged (Centrifuge 5415 R, Eppendorf) at 7,400 × *g* for 5 min at 4°C. The supernatant was discarded. The RNA pellet was air dried for 5-10 min at room temperature inside a fume cupboard and resuspended in 20 µL of 1X TE buffer (pH 8.0). The purity of the RNA extracted was quantified with Nanodrop ND-1000 spectrophotometer. The remaining RNA sample was stored at −80°C.

2.2.4.3 TRIzol RNA Extraction – Antimycin A Dose-Response Assays (1)

Each triplicate, containing 1 mL of THP-1 cells (~5×10^4 cells/mL per well) from the 24-well plate were centrifuged (Centrifuge 5415 R, Eppendorf) at 2000 × *g* for 7 min. The cell pellets were resuspend in 500 µL TRIzol and incubated at 15-30°C for 5 min. 100 µL of chloroform was added, shaken vigorously by hand for 15 sec and incubated at 15-30°C for 3 min. The mixture was centrifuged (Centrifuge 5415 R, Eppendorf) at 12,000 × *g* for 15 min at 4°C. The upper colourless RNA layer was transferred to a new RNase-free tube, with the triplicates from the same antimycin A concentration combined into one RNase-free tube. 500 µL of isopropanol was added to precipitate the RNA. The content was incubated at 15-30°C for 10 min and at −20°C for 20 min. This was then centrifuged (Centrifuge 5415 R, Eppendorf) at 12,000 × *g* for 10 min at 4°C. The supernatant was carefully removed. The RNA pellet was washed with 1 mL of 75% ethanol made with 0.01% DEPC water, mixed thoroughly by vortex and, centrifuged (Centrifuge 5415 R, Eppendorf) at 7,400 × *g* for 5 min at 4°C. The supernatant was discarded. The RNA pellet was air dried for 5-10 min at room temperature inside a fume cupboard and resuspended in 20 µL of 1X TE buffer (pH 8.0). The purity of the RNA extracted was quantified with Nanodrop ND-1000 spectrophotometer. The remaining RNA sample was stored at −80°C.

2.2.4.4 TRIzol RNA Extraction – Antimycin A Dose-Response Assays (2)

3 mL of THP-1 cells (~5×10^5 cells/mL) from the 6-well plate were centrifuged (Centrifuge 5415 R, Eppendorf) at 2000 × *g* for 7 min. The cell pellet was resuspend in 1 mL TRIzol. After resuspension, the TRIzol solution with pellet was transferred to sterile 1.5 mL Eppendorf tubes then incubated at 15-30°C for 5 min. 200 µL of chloroform was added, shaken vigorously by hand for 15 sec and incubated at 15-30°C for 3 min. The mixture was centrifuged (Centrifuge 5415 R, Eppendorf) at 12,000 × *g* for 15 min at 4°C. The upper colourless RNA layer was transferred to a new RNase-free tube. 500 µL of isopropanol was added to precipitate the RNA. The content was incubated at 15-30°C for 10 min and at −20°C for 20 min. This was then centrifuged (Centrifuge 5415 R, Eppendorf) at 12,000 × *g* for 10 min at 4°C. The supernatant was carefully removed. The RNA pellet was washed with 1 mL of 75% ethanol made with 0.01% DEPC water, mixed thoroughly by vortex and, centrifuged (Centrifuge 5415 R, Eppendorf) at 7,400 × *g* for 5 min at 4°C. The supernatant was discarded. The RNA pellet was air dried for 5-10 min at room temperature inside a fume cupboard and resuspended in 20 µL of 1X TE buffer (pH 8.0). The purity of the RNA extracted was quantified with Nanodrop ND-1000 spectrophotometer. The remaining RNA sample was stored at −80°C.

2.2.5 DNase Treatment of Total RNA

The DNase treatment kit used was obtained from Invitrogen. The following components were prepared in an RNase-free tube.

Table 7: Components used for DNase treatment

RNA	1 μg
10X Buffer	1 μL
DNase I (1 U/μL)	1 μL
0.01% DEPC H_2O	made up to **10 μL**

The tube was incubated at 37°C for 15 min. 1 μL of 25 mM EDTA was added as an exonuclease inhibitor. The solution was incubated at 65°C for 15 min to inactivate DNase I and returned to ice for 1 min. The product was collected by centrifugation at 7,400 × *g* for 20 sec (Centrifuge 5415 R, Eppendorf) and stored at −80ºC.

2.2.6 Formaldehyde Reducing Gel Electrophoresis

2.2.6.1 Preparation of 10X MOPS Buffer (pH 7)

3-(N-morpholino) propanesulfonic acid (MOPS) is a detergent that maintains the RNA integrity during electrophoresis. 400 mM of MOPS (AppliChem), 100 mM of

sodium acetate (Ajax Chemicals) and 10 mM of EDTA (BDH Laboratory Supplies) were dissolved in 0.01% DEPC water. The pH was adjusted to 7 then made up to 1 L with 0.01% DEPC water.

2.2.6.2 Preparation of 1% Reducing Gel

72 mL of 0.01% DEPC water was added to 1 g of agarose powder. The slurry was heated in a microwave to completely dissolve the agarose. 18 mL of 37% formaldehyde was added to the molten agarose solution and thoroughly mixed to make a 1% reducing gel. The gel was poured to be between 2-3 mm thick to give the best resolution. The addition of formaldehyde and the subsequent gel pouring were done in a fume hood.

2.2.6.3 Sample Preparation

The ingredients listed in Table 8 were added into an RNase-free tube for each sample.

Table 8: Components of each sample for formaldehyde reducing gel electrophoresis

RNA	1 μg
10X MOPS Buffer	2.5 μL
37% Formaldehyde	3.5 μL
Deionised Foramide (Sigma)	10 μL
Ethidium Bromide (10 mg/mL Sigma)	1 μL
Ficoll Gel Loading Dye	2 μL

The mixture was heated at 65°C for 15 min, returned on ice for 2 minutes then collected by brief centrifugation (Centrifuge 5415 R, Eppendorf).

2.2.6.4 Electrophoresis of RNA on Formaldehyde Reducing Gel

The entire sample mixture was loaded and run with 1X MOPS buffer (pH 7.0) at 100 V for 60 min. The gel was viewed under a UV illuminator/camera (Bio-Imaging Systems Ltd., DNR MiniBis Pro).

2.2.7 cDNA Synthesis with Reverse Transcriptase (RT)

For each RNA sample, PCR-graded water (Invitrogen), 1 μg of RNA and 1 μL of Oligo(dT) were incubated at 65ºC for 10 minutes to linearise the secondary RNA structures before the actual cDNA synthesis (Invitrogen kit). After denaturation, 4 μL of 5X RT buffer, 0.5 μL of RNase Inhibitor, 0.5 μL of RT (Invitrogen) and 2 μL of 10 mM dNTP were added to each RNA sample then incubated at 55ºC for 30 minutes. The RT activity was terminated by incubating at 85ºC for 5 minutes. A negative control with the RNA substituted by PCR-graded water was included. The cDNA was stored at −20ºC.

2.2.8 Polymerase Chain Reaction (PCR)

2.2.8.1 PCR – Trial

Polymerase chain reactions were used to amplify DNA fragments of certain sizes (section 2.1.5). A house-keeping gene, human glyceraldehyde 3-phosphate dehydrogenase, GAPDH was used to compare the expression differences of human hsp60 and TNF-α. The PCR components and the 0.2 mL nuclease-free tubes were purchased from Invitrogen. The volumes and final concentrations of the components are listed in Table 9. The cDNA control was used in the PCR as negative controls.

Table 9: Volumes and concentrations of PCR components developed by co-workers

Component	1× (µL), GAPDH and Hsp60	Component	1× (µL), TNF-α
cDNA	1	cDNA	0.5
PCR buffer (1 mM $MgCl_2$ finally)	2.5	PCR buffer (1 mM $MgCl_2$ finally)	2.5
dNTP	0.5	dNTP	0.5
forward primer (20 pmol)	0.25	forward primer	0.5
reverse primer (20 pmol)	0.25	reverse primer	0.5
Taq Polymerase (5 U/µL)	0.2	Taq Polymerase	0.2
PCR water	19.3	PCR water	20.3
Total	25	Total	25

Table 10: PCR conditions developed by co-workers

<table>
<tr><th>Product</th><th>Initial Denaturation</th><th>Denaturation</th><th>Annealing</th><th>Extension</th><th>Cycles of bold parts</th><th>Final Extension</th></tr>
<tr><td>GAPDH</td><td rowspan="3">95°C, 4 min</td><td rowspan="3">95°C, 1 min</td><td>60°C, 1 min</td><td rowspan="3">72°C, 1 min</td><td rowspan="2">24</td><td rowspan="3">72°C, 10 min</td></tr>
<tr><td>Hsp 60</td><td>55°C, 1 min</td></tr>
<tr><td>TNF-α</td><td>60°C, 1 min</td><td>29</td></tr>
</table>

2.2.8.2 PCR – After Antimycin A Dose-Response Assays

As the TNF-α bands from normal THP-1 cells were very faint on 2% agarose gels, one PCR condition for the dose-response assays, TNF cDNA volume, was changed from 0.5 μL to 1 μL per sample, together with the decrease of respective water volume. This is to ensure the visibility of all PCR products on 2% agarose gels, if one gene of interest is down-regulated after the antimycin A treatment.

Table 11: Volumes and concentrations of PCR components developed by co-workers

Component	1× (µL), GAPDH and Hsp60	Component	1× (µL), TNF-α
cDNA	1	cDNA	1
PCR buffer (1 mM $MgCl_2$ finally)	2.5	PCR buffer (1 mM $MgCl_2$ finally)	2.5
dNTP	0.5	dNTP	0.5
forward primer (20 pmol)	0.25	forward primer	0.5
reverse primer (20 pmol)	0.25	reverse primer	0.5
Taq Polymerase (5 U/µL)	0.2	Taq Polymerase	0.2
PCR water	20.3	PCR water	19.8
Total	25	Total	25

Table 12: PCR conditions used for antimycin A dose-response assays

Product	Initial Denaturation	**Denaturation**	**Annealing**	**Extension**	Cycles of **bold** parts	Final Extension
GAPDH	95°C, 4 min	**95°C, 1 min**	**60°C, 1 min**	**72°C, 1 min**	24	72°C, 10 min
Hsp 60			**55°C, 1 min**			
TNF-α			**60°C, 1 min**		29	

2.2.9 Non-reducing Agarose Gel Electrophoresis

2.2.9.1 Preparation of 2% Agarose Gel

Non-reducing agarose gel electrophoresis was used to separate DNA fragments of different sizes. 2 g of agarose powder was mixed with 100 mL of 1X SB buffer (pH 8.5). The slurry was heated in a microwave oven till thoroughly melted. 2.5 μL of 10 mg/mL ethidium bromide was added to the molten agarose. The agarose solution was cooled to approximately 60ºC then poured into either three mini-gel trays (Owl B1A) or a large one (Owl B2) and allowed to solidify.

2.2.9.2 Separation of PCR Products on Non-Reducing Agarose Gel

The 3 μL of each PCR products plus 2 μL gel loading dye (Ficoll) were thoroughly mixed and loaded and run on a 2% agarose gel in 1X SB buffer (pH 8.5), at 80V for 60 minutes. The agarose gel was viewed under a UV illuminator/camera (Bio-Imaging Systems Ltd., DNR MiniBis Pro). A photo of the gel image was taken for band intensity analysis. In order to produce the highest possible resolution for intensity analysis, all electrophoresis photos were saved as .tif files.

2.2.9.3 Quantitation of PCR Products with Gel Quant

The area of the gel bands were calculated using Gel Quant software (DNR Imaging Systems Ltd., Gel Quant 2.7.0). To do so the Object Borders, Object Centres and Standards were firstly selected to be on. Both lanes and bands were analysed. The band areas were then adjusted to fit the actual bands. The calculated table of band areas was exported to a Microsoft Excel Workbook, after all the band areas were adjusted. The ratio of target gene expression/house keeping gene expression was further calculated.

2.2.10 Statistical Analysis

Tukey Multiple Comparisons of Means was applied to data from antimycin A dose-response assays (2.2.2.1 and 2.2.2.2) using statistical programme R.

CHAPTER THREE

ESTABLISHING A THP-1 CELL LINE WITH COMPROMISED MITOCHONDRIAL FUNCTIONS

3.1 Normal Growth of THP-1 Cells

The THP-1 cell growth in normal RPMI 1640 medium is illustrated in Figure 1. After an initial lag phase from Day 0 to Day 1, there was a steady increase of approximately 2×10^4 cells per day.

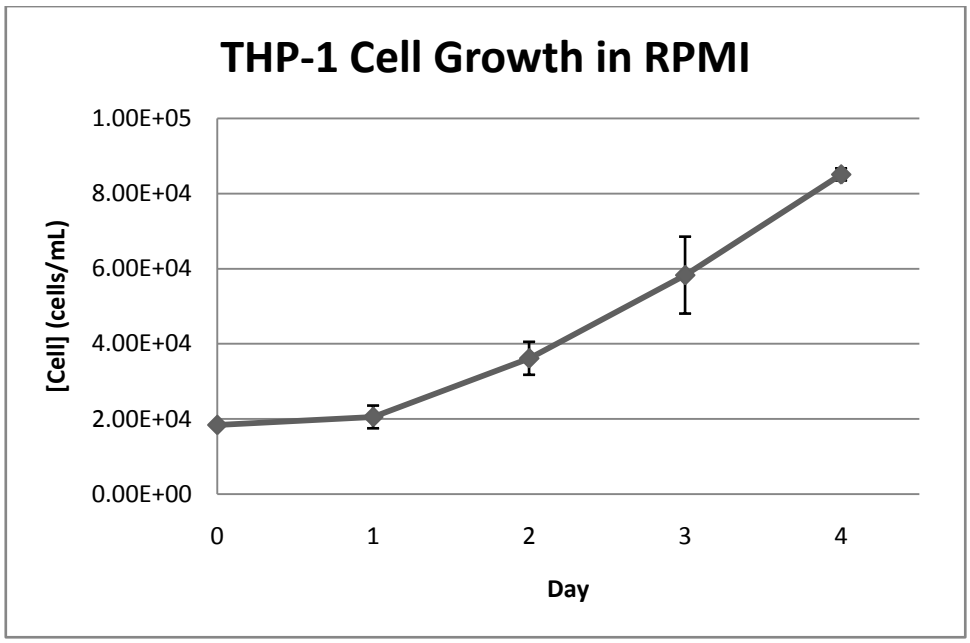

Figure 1: THP-1 cells grown in standard liquid medium (n = 3).

Each error bar represents one standard deviation.

3.2 THP-1 Cell Growth in Normal Medium plus Ethanol

Since the mitochondrial inhibitor used in this assay, antimycin A, was dissolved in ethanol, the effect of this solvent on the growth of THP-1 monocytes was investigated. Figure 2 indicates that THP-1 cell growth was not affected by 5 μM of ethanol, but as the concentration increased from 10 μM to 200 μM, the growth rate gradually slowed down. For 5 μM of ethanol, the viable cell number was very similar to the untreated control across all five days (Figure 2). For 10, 25 and 50 μM of ethanol, there were approximately 10^4 cells less than the untreated control on Day 4, approximately 5000 cells less than the untreated control on Day 3, but no differences in viable cell

concentrations before Day 3 compared to the untreated control (Figure 2). For 100 and 200 μM of ethanol, there were approximately 2×10^4 less cells than the untreated control on Day 4, and approximately 10^4 less cells than the untreated control on Day 3 (Figure 2).

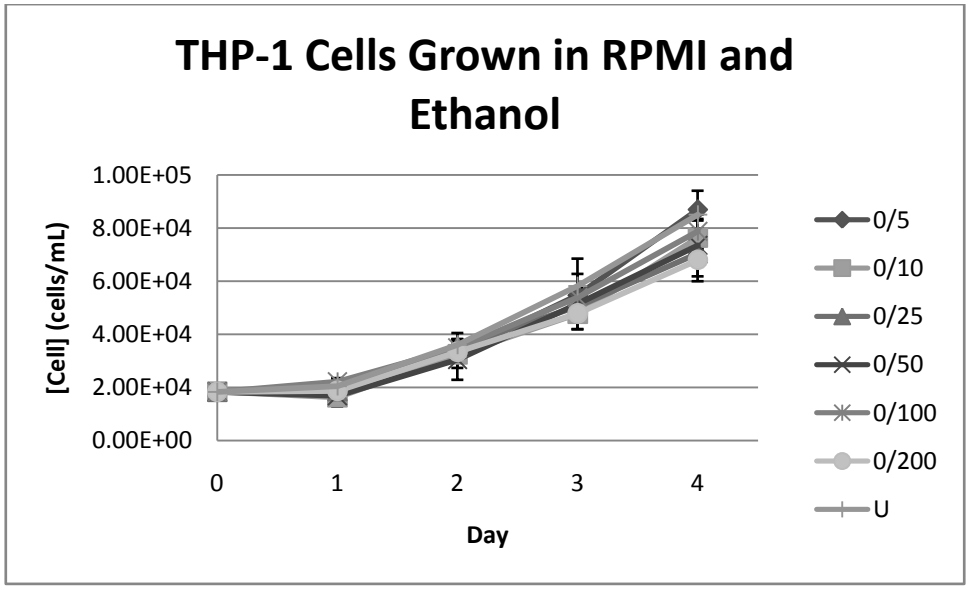

Figure 2:THP-1 cells maintained in RPMI medium containing 0 (U = untreated control), 5, 10, 25, 50, 100 or 200 μM of ethanol respectively (n = 3).

Each error bar represents one standard deviation.

3.3 Growth of THP-1 in the Presence of Antimycin A

The mechanism of antimycin A, as a Complex III inhibitor of electron transport system, was discussed in the literature review and associated method. It gave potent growth inhibitions to THP-1 cells at even 5 μM level. The inhibiting effect is

dependent on the concentration, compared to the untreated control. The conditioned growth medium of THP-1 monocytes treated with antimycin only was yellower than untreated and solvent controls. According to Figure 3, there was still some cell growth in 5 (approximately 2×10^4 more on Day 4 than Day 0) and 10 μM (approximately 10^4 more on Day 4 than Day 0) of antimycin A, although the rate was severely restricted. Cells in 25 and 50 μM of antimycin A remained viable but could not grow to increase the population; whereas ones in 100 and 200 μM of antimycin A only decreased because the levels of inhibitor were too toxic (Figure 3).

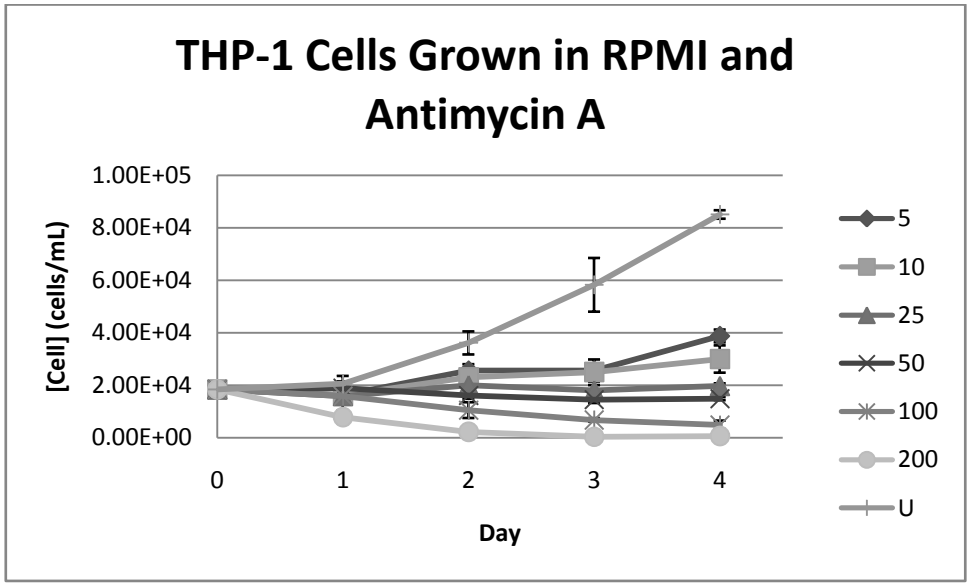

Figure 3: THP-1 cells maintained in RPMI medium containing 0 (U, untreated control), 5, 10, 25, 50, 100 or 200 μM of antimycin A respectively (n = 3).

Each error bar represents one standard deviation.

A comparison of untreated and solvent controls against respective antimycin A concentrations (Figure 4) shows that the severe inhibition of THP-1 cell-growth in the presence of antimycin A is not due to the solvent, even though the growth rate slightly decreased if ethanol is present, as discussed in 3.2.

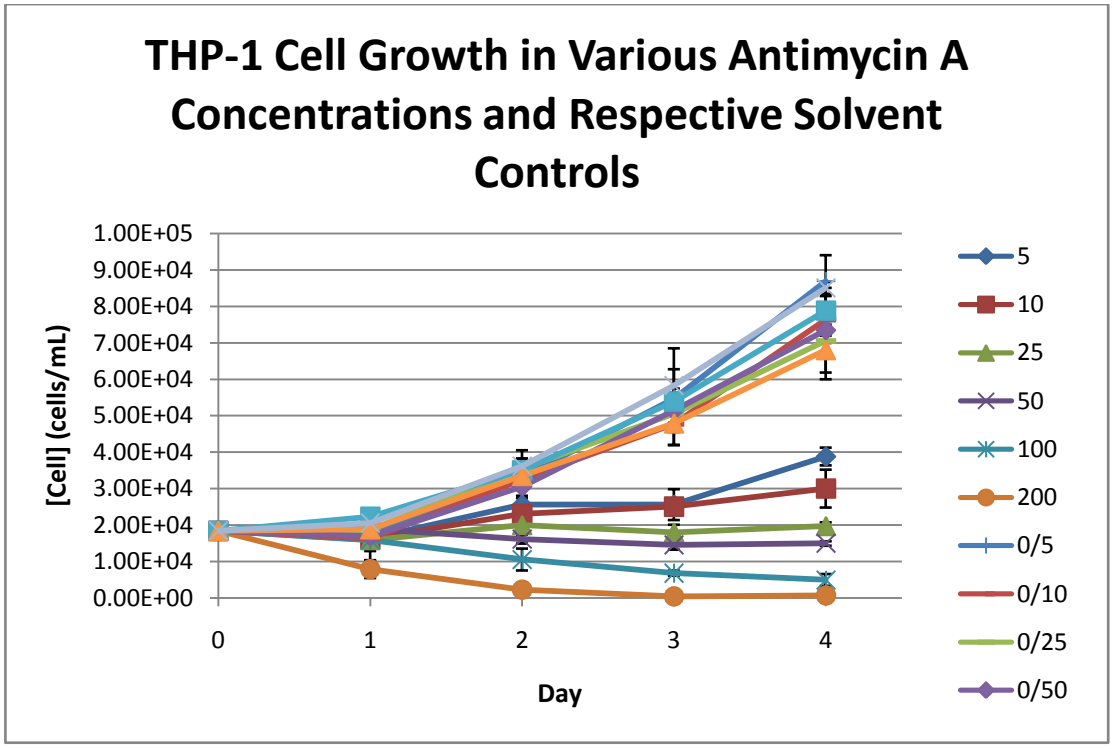

Figure 4: THP-1 cells grown in media containing various antimycin A concentrations compared with respective controls (n = 3).

U = untreated control. Each error bar represents one standard deviation.

3.4 Redox Rescue

In order to see if the growth inhibitory effect of antimycin A could be overcome or ameliated by redox rescue agents, THP-1 monocytes were grown in the presence of pyruvate and uridine. 50 μg/mL uridine and 1 mM sodium pyruvate were included in the media for pyrimidine biosynthesis (uridine) and redox sink molecule or redox rescuer (pyruvate) as discussed in 2.2.2.2, combining with 5, 10, 25, 50, 100 or 200 μM of antimycin A respectively. The conditioned growth medium of THP-1 monocytes treated with antimycin A, uridine and pyruvate was yellower than respective untreated and solvent controls. Yet it was as yellow as the cells having antimycin A only. Uridine and pyruvate allowed the viable cell numbers in 5, 10, 25 and 50 μM of antimycin A to multiply faster than the cells without (Figure 5). 100 and 200 μM of antimycin A were still too toxic to THP-1 cells so they rapidly deceased (Figure 5).

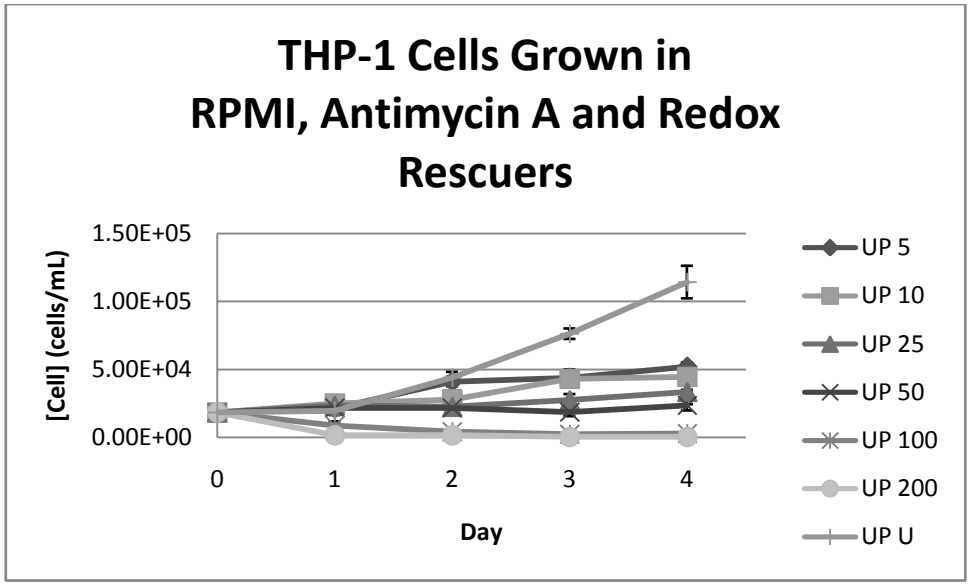

Figure 5: THP-1 cells maintained in RPMI medium containing 50 µg/mL uridine, 1 mM sodium pyruvate, together with 0 (U, untreated control), 5, 10, 25, 50, 100 or 200 µM of antimycin A respectively (n = 3).

Each error bar represents one standard deviation.

A comparison of untreated and solvent controls against various concentrations of antimycin A in the presence of uridine and pyruvate (Figure 6) shows that the severe cell-growth inhibition is not due to the solvent, either; although there were slight decreases in growth rates compared to the untreated control when ethanol was present.

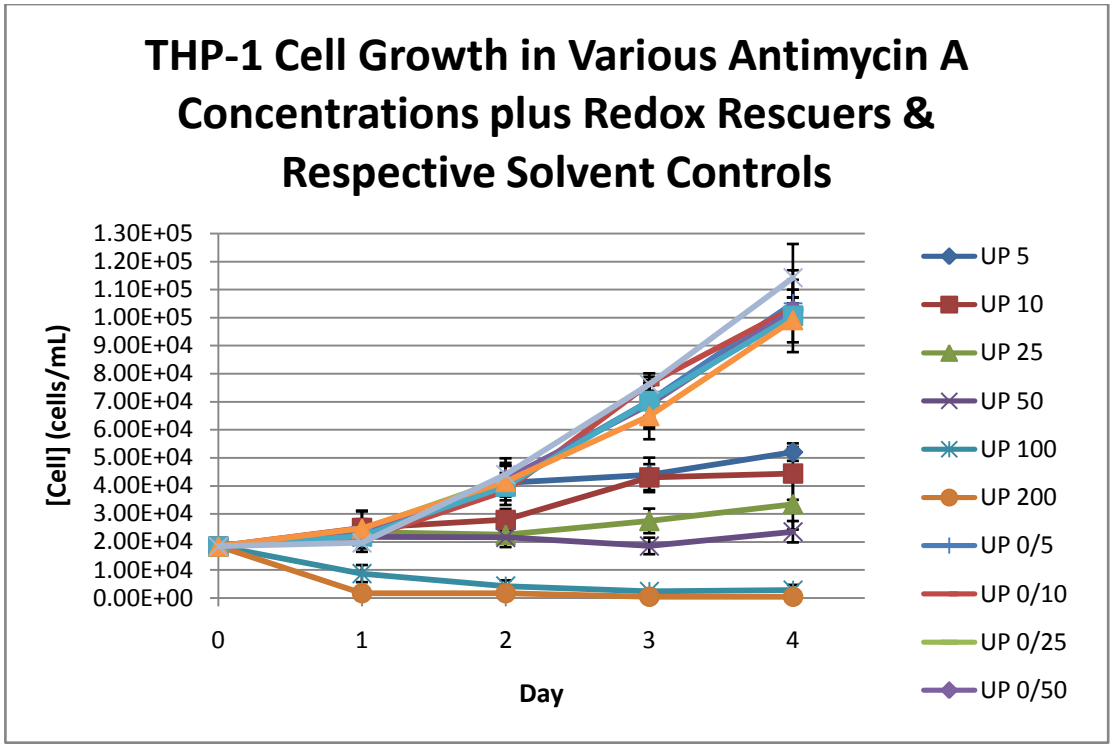

Figure 6: THP-1 cells grown in media containing various antimycin A concentrations including redox rescuers, compared with respective controls (n = 3).

U = untreated control. Each error bar represents one standard deviation.

3.5 Statistical Analyses

The results of antimycin A dose-response assays were analysed by Tukey Multiple Comparisons of Means. This kind of statistical test was performed because more than two variables were compared, which *t* test would not suit. The analysed results were illustrated in Table 13 in terms of *p* values. THP-1 monocytes treated with uridine and pyruvate were not significantly different from corresponding ones without,

including their solvent controls compared to respective untreated controls. However, the antimycin A treated samples were significantly different from their respective solvent and untreated controls. This is the same when uridine and pyruvate were added. Solvent controls were not significantly different compared to untreated controls in all parameters.

Table 13: *p* values obtained from each antimycin A concentrations using Tukey Multiple Comparisons of Means.

Red figures indicated no statistical significance (*p* value > 0.05).

p value of Tukey Multiple Comparisons of Means	[Antimycin A] (μM)					
	5	10	25	50	100	200
AA only solvent vs AA	0.0000213	0.0000856	0.0002483	0.0000002	0.0000000	0.0000005
AA only U vs AA	0.0000319	0.0000150	0.0000204	0.0000000	0.0000000	0.0000000
AA vs AA + UP	0.2466417	0.2583839	0.4948712	0.4348168	0.9973485	1.0000000
AA only U vs AA only solvent	0.9993070	0.7290985	0.4385034	0.1779117	0.7829941	0.0786210
UP solvent vs AA + UP	0.0000077	0.0000074	0.0000119	0.0000000	0.0000000	0.0000000
UP U vs AA + UP	0.0000014	0.0000012	0.0000021	0.0000000	0.0000000	0.0000000
UP U vs UP solvent	0.5910283	0.5219193	0.6242867	0.1779117	0.1233147	0.1406779

Table 14: Legend for Table 13

Legend	Description
AA	Antimycin A without uridine, pyruvate
AA only solvent	Solvent control without uridine, pyruvate
AA only U	Untreated control without uridine, pyruvate
AA + UP	Antimycin A plus uridine, pyruvate
UP solvent	Solvent control plus uridine, pyruvate
UP U	Untreated control plua uridine, pyruvate

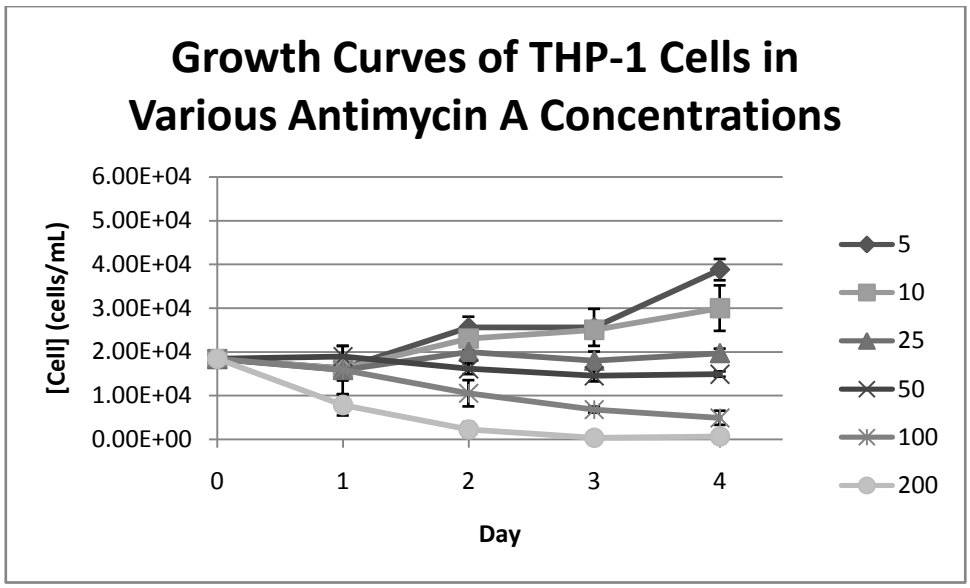

Figure 7: Antimycin A inhibition of THP-1 cell-growth plotted on the scale as Figure 8.

Each error bar represents one standard deviation (n = 3). Figures 7 and 8 are to compare the THP-1 cell growth with or without uridinen pyruvate.

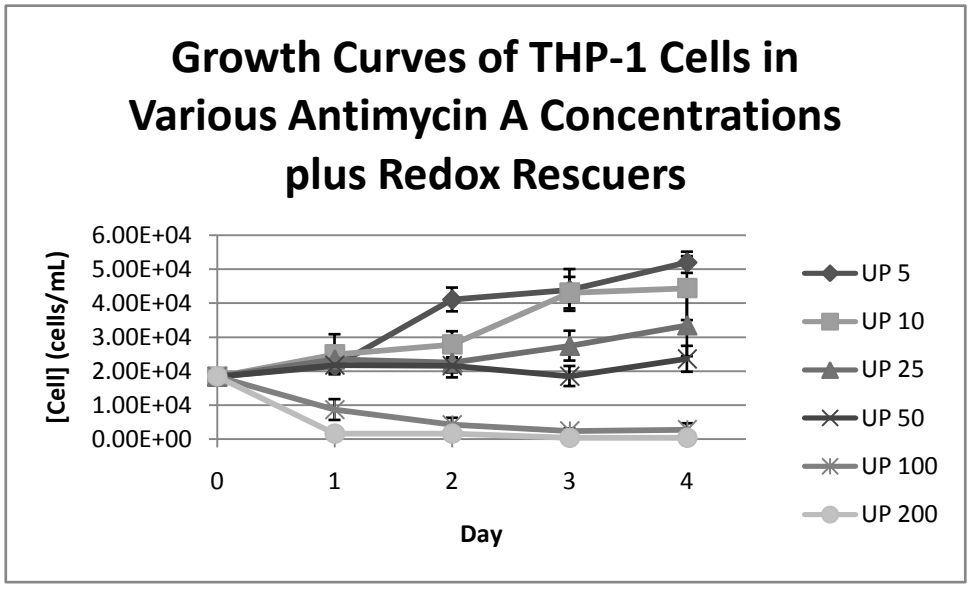

Figure 8: Antimycin A inhibition of THP-1 cell-growth with the help of redox rescuers. Each error bar represents one standard deviation (n = 3).

CHAPTER FOUR TOTAL RNA EXTRACTION

4.1 Trials of TRIzol RNA Extractions

The detailed protocols of extracting total RNA from THP-1 monocytes were described in 2.2.4. A good RNA extraction is defined by three criteria: RNA quantity, purity and integrity. These determine if the extracted RNA is at the optimal condition and applicable for follow-on experimental work. The quantity of RNA needed varies from assays to assays. For example, the detection of RNA integrity using formaldehyde reducing gel requires at least 500 ng of total RNA; however only 10 ng to 5 μg of RNA is enough for cDNA synthesis (Roche). RNA purity is commonly measured by the spectrophotometric absorbance ratio of 260/280 nm ($A_{260/280}$). RNA samples free from protein and DNA contaminations generally give $A_{260/280}$ from 1.9 to 2.1.

Yet an acceptable $A_{260/280}$ ratio gives no indications that the RNA extracted is still intact. A highly pure RNA sample can be totally degraded into pieces that although enough added to cDNA synthesis and PCR, no useful results can be obtained. The

integrity of mammalian RNA is defined by two distinct bands of 18S and 22S ribosomal RNA (rRNA) when separated by formaldehyde reducing gel electrophoresis. These rRNA compose of approximately 50% of the total RNA in mammalian cells. If the RNA is degraded, a smear instead of distinct bands, along the track would be expected on a formaldehyde gel after electrophoresis.

4.1.1 TRIzol RNA Extraction – Attempt One

THP-1 monocyte cells grown in normal growth medium were used to ensure the extraction protocol was applicable for this project. Four random samples (THP-1 R1−R4) from the same culture flask were used. The volumes of these samples were all 1 mL with concentrations approximately 10^5 cells/mL. The method used was illustrated in 2.2.4.1. The $A_{260/280}$ ratios of these RNA samples were 1.21−1.78, rather than 1.9−2.1. This shows that the RNA was impure.

Table 15: The first attempt of TRIzol RNA extraction

Sample ID	ng/μL	260/280
THP-1 R1	277.92	1.21
THP-1 R2	181.07	1.21
THP-1 R3	1027.1	1.78
THP-1 R4	153.88	1.51

4.1.2 TRIzol RNA Extraction – Attempt Two

After comparing with another protocol of RNA extraction from mammalian cells (Sambrook et al. 1989), it suggested that centrifuging at 13,000 rpm would lyse cells, thus losing RNA into supernatant. RNase stored in cells could be released therefore degrading some RNA. Moreover, precipitating RNA at room temperature may not be enough. This means further precipitation at −20ºC for 20 minutes could be needed. After several practices (data not shown) of the protocol in 2.2.4.3 the $A_{260/280}$ ratios were finally within 1.9 and 2.1 (THP-1 R5.1−5.4) with good yield (565.80−1670.7 ng/μL) were obtained.

1 μg of linear RNA from each sample was visualised under a UV illuminator/camera (DNR Imaging Systems, Minibis Pro). According to the reducing gel electrophoresis,

RNA samples were all intact and the amount was improved from Attempt One (Figure 9, -10 and Table 16). Although some smears still existed, 18S and 22S rRNA bands from samples THP-1 R5.1−5.4 carried according to the protocol described, were clearly distinct (Figure 9). Since the extracted RNA was intact, DNase treatment was followed.

Table 16: The acceptable yield of total RNA extraction with TRIzol

Sample ID	ng/µL	260/280
THP-1 R5.1	565.80	1.98
THP-1 R5.2	534.91	1.98
THP-1 R5.3	1075.1	2.00
THP-1 R5.4	1670.7	1.98

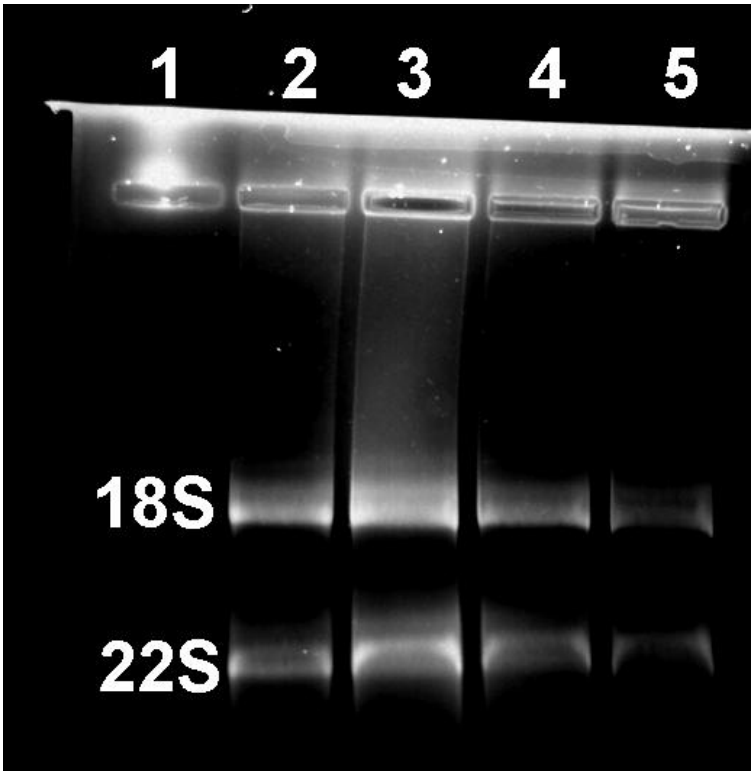

Figure 9: Total RNA extracted from THP-1 cells using TRIzol was run on a 1% formaldehyde reducing gel, before DNase treatment.

The top band represented 18S rRNA, while the bottom indicated 22S rRNA. Lane 1 = blank, as the standard RNA was eliminated due to its old age; Lane 2−5 = RNA samples THP-1 R5.1−5.4. The RNA was intact, despite of some remaining contaminations as shown by the smears.

RNA samples, THP-1 R5.1−5.4, were treated with DNase I (Invitrogen) using the protocol listed in 2.2.5. After DNase treatment, 1 μg of each RNA sample was run on 1% formaldehyde reducing gel and viewed under a UV illuminator (DNR Imaging Systems Ltd., MiniBis Pro). The RNA samples were all intact, especially the

impurities were removed during DNase treatment, as indicated by less smears on each lane (Figure 10).

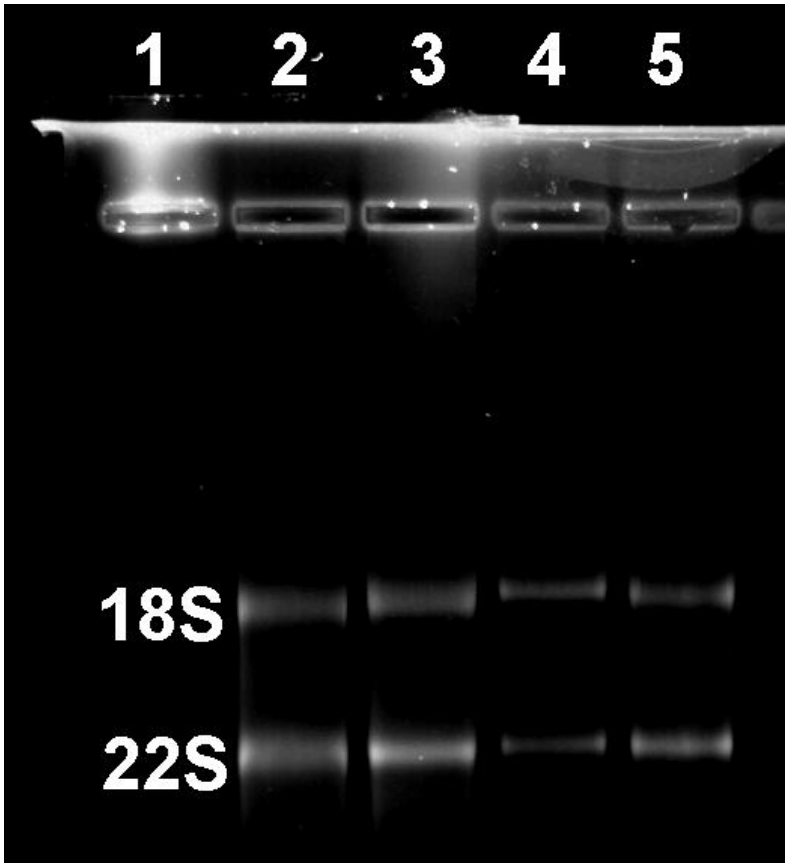

Figure 10: After DNase treatment, 1 µg of RNA extracted from THP-1 cells using TRIzol was run on a 1% formaldehyde reducing gel.

Lane 1 = blank; Lane 2−5 = RNA samples from THP-1 R5.1−5.4, the four random samples taken from cells grown in the same flask with standard growth medium. Contaminating DNA was taken away as the smears on the running tracks shown in Figure 9 disappeared.

4.2 RNA Extraction after Antimycin A Dose-Response Assays

4.2.1 Attempt One

The method of challenging THP-1 monocytes with various antimycin A concentrations was mentioned in 2.2.3. Total RNA extraction (protocol 2.2.4.3) using TRIzol (Invitrogen) was done after antimycin A challenge. Approximately 5×10^4 cells/mL was used in each triplicate to extract total RNA. The extraction conditions and reagents used were identical as 2.2.4.2, except that 1 mL of suspended THP-1 cells from each triplicate was taken from each triplicate, and the RNA solution of triplicates with the same antimycin A concentrations were combined into one RNase-free tube.

The RNA yields obtained after antimycin A treatment was not good with the first attempt, with $A_{260/280}$ ratios ranging from 1.37 to 1.86, and yield between 33.36 and 482.02 ng/μL. This could be due to the low viable cell concentration remained after five days of mitochondrial inhibitor challenge, since the $A_{260/280}$ ratios of solvent and untreated controls without uridine and pyruvate were still acceptable (Table 17). Using higher cell concentration at the initial stage of challenge was then attempted (protocol 2.2.3.2).

Table 17: RNA yield after TRIzol RNA extraction (1)

Sample ID	ng/µL	260/280	Sample ID	ng/µL	260/280
5 µM	146.99	1.79	UP 5 µM	81.4	1.46
10 µM	138.64	1.69	UP 10 µM	102.34	1.49
25 µM	304.75	1.70	UP 25 µM	134.48	1.66
50 µM	120.63	1.61	UP 50 µM	36.67	1.37
100 µM	106.26	1.41	UP 100 µM	71.08	1.41
200 µM	33.36	1.83	UP 200 µM	83.76	1.57
0/5 µM	337.72	1.98	UP 0/5 µM	276.01	1.72
0/10 µM	349.69	1.95	UP 0/10 µM	408.38	1.79
0/25 µM	384.53	1.86	UP 0/25 µM	458.53	1.86
0/50 µM	363.74	1.95	UP 0/50 µM	150.54	1.51
0/100 µM	393.60	1.91	UP 0/100 µM	482.02	1.72
0/200 µM	375.27	1.98	UP 0/200 µM	303.18	1.49
U	371.80	1.91	UP U	517.61	1.79

4.2.2 Attempt Two

The antimycin A challenge was repeated with THP-1 monocytes again, as explained in 2.2.3.2. For each replicate, the initial cell concentration was raised from 1.84×10^4 to 1×10^5 cells/mL. All cells were used to extract total RNA instead of just 1 mL. The purity and yield of the second attempt were much better than the first one (Table 18). All $A_{260/280}$ ratios reached above 1.9, plus the yield ranged from 566.00 to 3430.0 ng/μL; apart from cells grown in 25 and 50 μM of antimycin A. The low purity and yield of these two replicates could be due to the few viable cells surviving after five days of antimycin A treatment (Table 18).

Table 18: RNA yield after TRIzol RNA extraction (2)

Sample ID	ng/µL	$A_{260/280}$	Sample ID	ng/µL	$A_{260/280}$
5 µM	1150.2	2.03	UP 5 µM	1399.8	2.03
10 µM	1593.0	2.02	UP 10 µM	1573.2	2.03
25 µM	20.69	1.53	UP 25 µM	828.67	2.03
50 µM	6.53	1.36	UP 50 µM	566.00	1.94
U	3430.0	1.94	UP U	3255.5	1.95

The RNA was further purified with DNase using the protocol listed in 2.2.5. 1 µg of these DNase-treated RNA was then run on 1% formaldehyde reducing gel (protocol 2.2.6). The results after reducing gel electrophoresis are in Figure 11 and Figure 12. All RNA was intact and present in good quantity for samples UP 5−50 µM, which were extracted from THP-1 cells exposed to 5−50 µM antimycin A plus uridine and pyruvate. Yet the RNA from 10 µM antimycin A treatment was degraded immediately after extraction; plus the yield from 25 and 50 µM were very low (Figure 11). Also some RNA from the untreated sample (U) degraded, as shown at the bottom of the formaldehyde gel (Figure 11). Despite so, these DNase-treated RNA was still used for cDNA synthesis and PCR, as most of the extractions worked well.

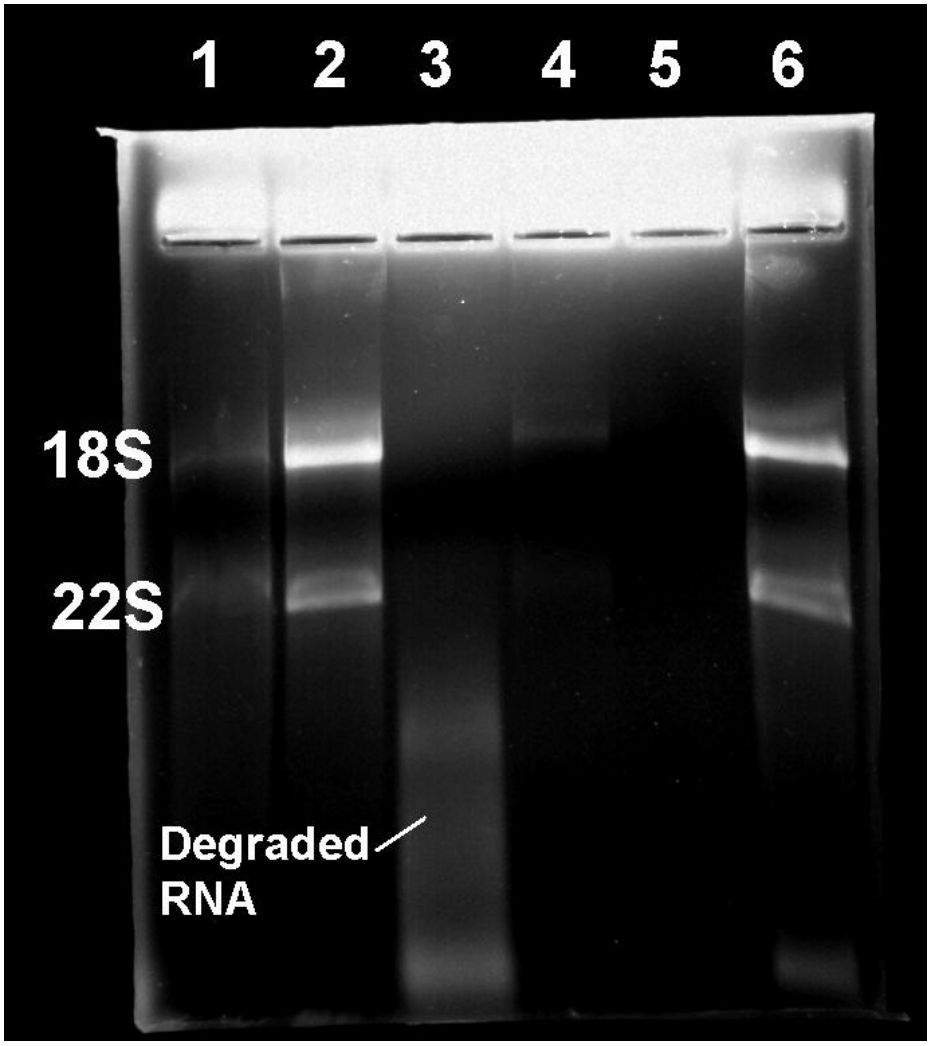

Figure 11: Reducing gel showing total RNA extracted from THP-1 cells after five days of antimycin A treatment, after DNase treatment.

Lane 1 = 18S + 22S standard rRNA (Sigma); Lane 2−Lane 5 = 5, 10, 25, 50 μM antimycin A and Lane 6 = untreated control (U). RNA from THP-1 cells grown in 10 μM antimycin A was degraded instantly after extraction. This is why no bands could be seen in Lane 3 but with a smear at the lower part of the gel instead. RNA from THP-1 cells grown in 25 μM antimycin A had lower yield, so the bands were very faint on a reducing gel. RNA amount from THP-1 cells grown in 25 μM antimycin A

was even worse; therefore no bands could be detected. Some contaminations, possibly from DNA, are still present at the top of each well.

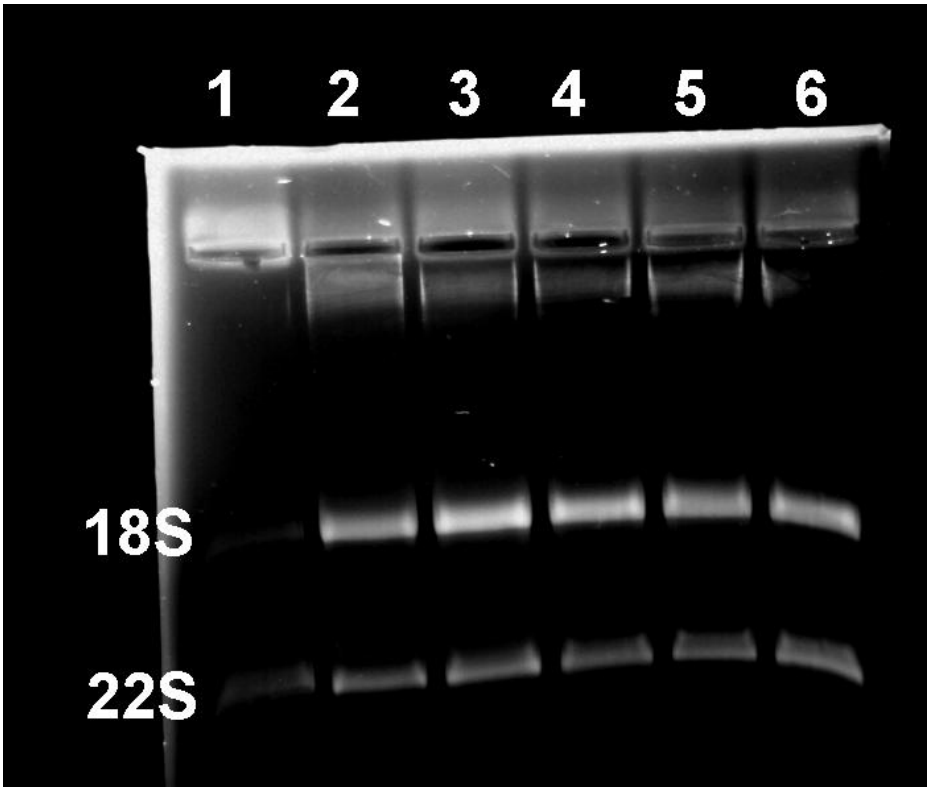

Figure 12: Reducing gel showing total RNA extracted from THP-1 cells after five days of antimycin A plus uridine and pyruvate treatment (denoted as UP), after DNase treatment.

Lane 1 = 18S + 22S standard rRNA (Sigma); Lane 2 = UP 5; Lane 3 = UP 10; Lane 4 = UP 25; Lane 5 = UP 50 μM antimycin A and Lane 6 = UP untreated control (UP U).

CHAPTER FIVE REVERSE TRANSCRIPTASE-POLYMERASE CHAIN REACTION (RT-PCR)

The polymerase chain reaction (PCR) was invented by Kary Mullis in 1980 (Wikowski & Zoller, 2001) as a technique of replicating certain regions of DNA. It is sensitive enough to amplify from very small amount of DNA templates. PCR has extremely wide applications in laboratories because of its efficient and straight forward operation.

In a generic PCR process, a piece of double-stranded DNA is first denatured at 94ºC for five minutes to become linear, single-stranded DNA. Oligonucleotide primers are used as starting points of replications. These primers have specific sequences so they can anneal to the beginning and the end of a DNA fragment or region. The annealing temperature varies from gene to gene, but is generally between 50 and 60ºC. After annealing, an extension step is used by adding single nucleotides (dNTP) between the

forward (from the beginning) and the reverse (from the end) primers with the help of a heat resistant enzyme, Taq polymerase. The temperature for extension is approximately 72ºC. With 25−40 replicating cycles one can generate enough DNA copies that are detectable via non-reducing agarose gel electrophoresis.

The precise PCR conditions depend on different genes and sample types. Commonly adjusted conditions are: the amount of DNA template, Mg^{2+} concentration, annealing temperatures and number of cycles. Mg^{2+} concentration is crucial because the ion interacts with primers, affecting the annealing results of primers. The cycle number needs to be changed as not all templates exist in equal number of copies. In other words not all genes are expressed in the same intensity. For the ones that express more, more copies of associated mRNA is present in the total RNA. These genes are referred as “high copy number” genes. In contrast, for the “low copy number” genes, more replicating cycles are needed in order to visualise on agarose gel electrophoresis. However, one needs to make sure that the cycle number is not too many; otherwise the products will over-saturate the solution, causing it to be very viscous. This means that molecules are hard to move around in solution, so some of the procedures such as extension may be incomplete. In such circumstance, the gene expression level may not be accurately represented due to incomplete extension steps.

In this project, a constitutively expressed gene, or house keeping gene is used to show that the expression differences between genes are indeed due to different dose-response treatments, instead of operational or systematic errors. The expression can be stated as a ratio of target gene expression/house keeping gene expression.

5.1 RT-PCR Trial

RNA samples, 5.1−5.4 as mentioned in Table 16, were used to run RT-PCR trials to ensure that all reagents functioned appropriately (protocols 2.2.7 and 2.2.8.1). A house keeping gene, human glyceraldehydes 3-phosphate dehydrogenase (GAPDH), was used as a control to normalise the gene expression of human Hsp60 and TNF-α. The primer sequences of these three genes were listed in 2.1.8.

The PCR results were produced according to the optimised conditions developed by other co-workers. The band intensities for GAPDH and Hsp60 were within the visible range, yet the TNF-α bands were too faint (Figures 13 and 14). If the TNF-α expression is down-regulated in the antimycin A dose-response assay, the bands may be invisible. Thus the TNF-α cDNA volume was increased to 1 μL for the dose-response assays.

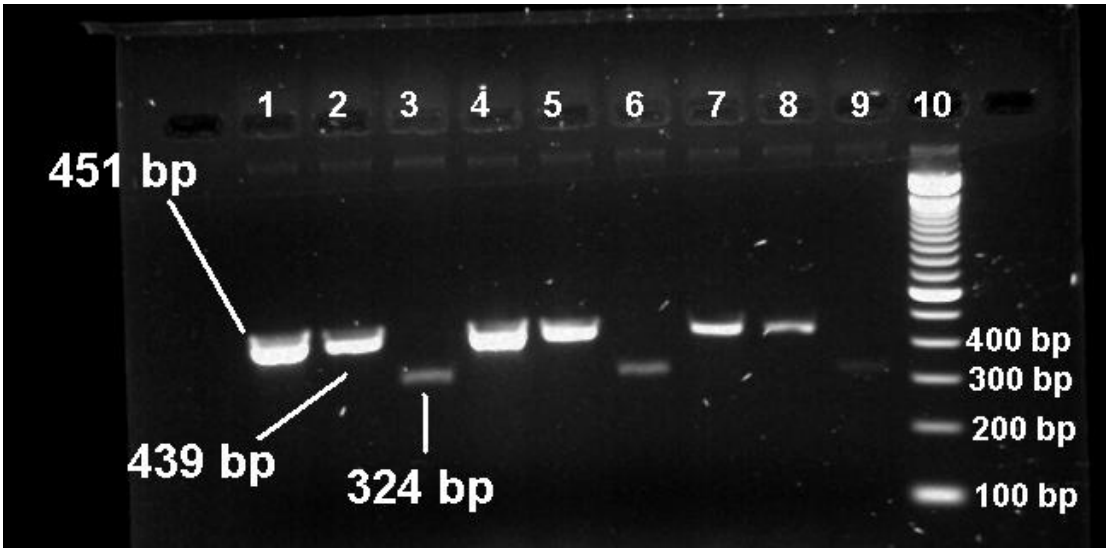

Figure 13: RT-PCR of GAPDH, Hsp60 and TNF-α.

Lane 1−3, GAPDH, Hsp60 and TNF-α (R5.1); Lane 4−6, GAPDH, Hsp60 and TNF-α (R5.2); Lane 7−9, GAPDH, Hsp60 and TNF-α (R5.3); Lane 10, 100 bp ladder.

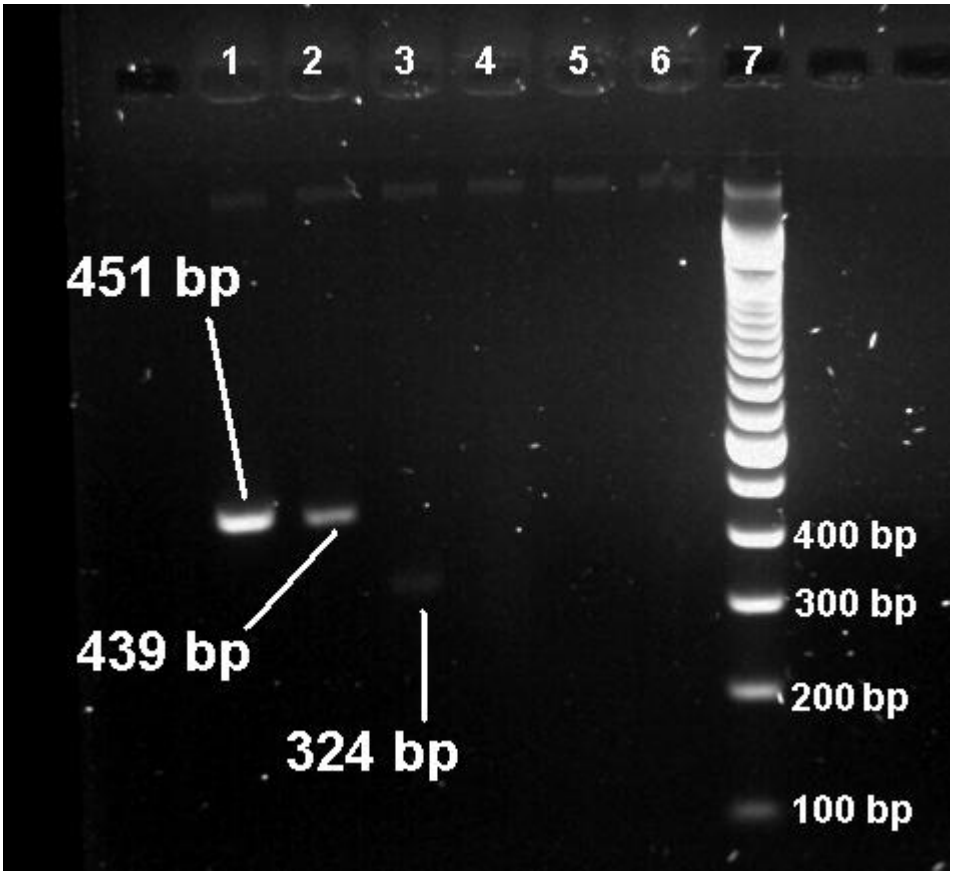

Figure 14: RT-PCR of GAPDH, Hsp60 and TNF-α with respective negative controls.

Lane 1−3, GAPDH, Hsp60 and TNF-α (R5.4); Lane 4−6, negative controls of GAPDH, Hsp60 and TNF-α PCR; Lane 7, 100 bp ladder.

5.2 RT-PCR After Antimycin A Dose-Response Assay

The RT-PCR results after antimycin A dose-response assay (2.2.3.2) and total RNA extraction (2.2.4.4) is shown in Figure 15. The detailed method is stated in 2.2.7 and 2.2.8.2. No detectable contaminations were observed according to the negative

controls of human GAPDH, Hsp60 and TNF-α PCR. Most of the PCR products were visible on the 2% non-reducing agarose gel, apart from samples 10 and 50 μM antimycin A only. No detectable products could be found for THP-1 monocytes grown in these two conditions. There were two reasons for such failed PCR. The RNA was found to be degraded after extraction (Figure 11) in sample 10 μM antimycin A only; and the purity as well as yield were too low for 50 μM antimycin A only (Table 18). According to Figure 15, GAPDH, Hsp60 and TNF-α expression was all down-regulated in response to increasing antimycin A concentration, when no uridine and pyruvate were added. When uridine and pyruvate were applied, GAPDH showed almost no change in expression in response to increasing antimycin A concentration; a slight up-regulation was observed in both Hsp60 and TNF-α. Notably, TNF-α expression was extremely low in antimycin A only conditions.

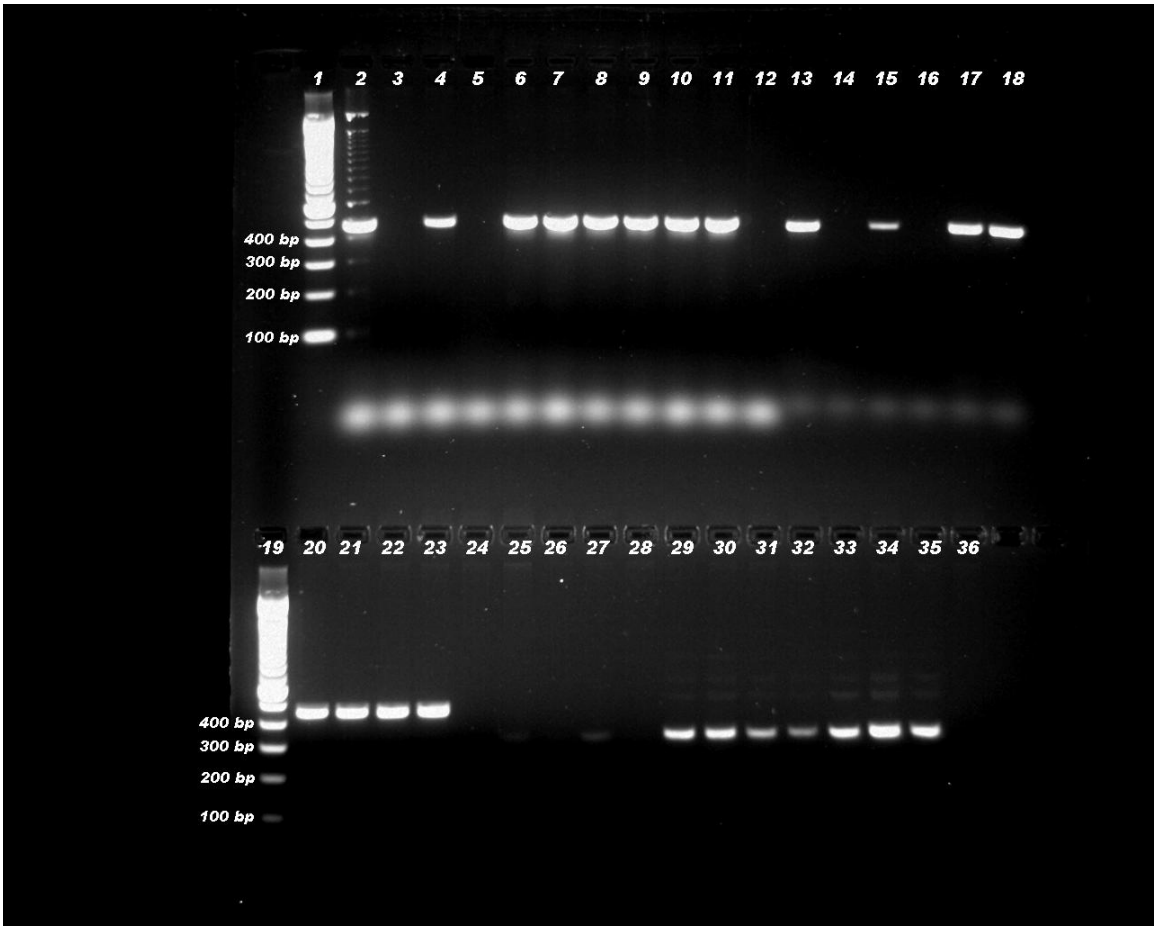

Figure 15: The RT-PCR products were run on a 2% non-reducing agarose gel.

Label starts from the top left: Lane 1, 100 bp ladder, Lane 2−5: GAPDH expression of 5, 10, 25, 50 μM antimycin A only; Lane 6, untreated control of antimycin A only; Lane 7−10 GAPDH expression of 5, 10, 25, 50 μM antimycin A plus uridine, pyruvate, Lane 11, untreated control of antimycin A plus uridine, pyruvate; Lane 12, negative control of GAPDH PCR; Lane 13−16, Hsp60 expression of 5, 10, 25, 50 μM antimycin A only, Lane 17, untreated control of antimycin A only; Lane 18−22 (excluding 100 bp ladder), Hsp60 expression of 5, 10, 25, 50 μM antimycin A plus uridine, pyruvate; Lane 23, untreated control of antimycin A plus uridine, pyruvate; Lane 24, negative control of Hsp60 PCR; Lane 25−28, TNF-α expression of 5, 10, 25, 50 μM antimycin A only; Lane 29, untreated control of antimycin A only; Lane

30−34, TNF-α expression of 5, 10, 25, 50 μM antimycin A plus uridine, pyruvate; Lane 35, untreated control of antimycin A plus uridine, pyruvate; Lane 36, negative control of TNF-α PCR. Lane 31 is a repeated loading from the same PCR product of TNF-α expression in 10 μM antimycin A plus uridine and pyruvate.

5.3 Quantification of Band Areas

The following description relates to Figures 16, -17 and Table 19. Ratios closer to one when compared against GAPDH indicate higher expression. UP-treated THP-1 monocytes had higher expression level of both Hsp60 and TNF-α in all antimycin A concentrations, including untreated controls, relative to the respective antimycin A only conditions. The expression of Hsp60 was more elevated than TNF-α in all antimycin A concentrations, including UP-treated and untreated controls. Hsp60 expression was down-regulated in response to increasing antimycin A concentration, compared to the untreated control. Yet this was reversed when uridine and pyruvate were added. 25 μM antimycin A with uridine and pyruvate (UP Hsp60 25), possibly an outlier, showed even higher expression of hsp60 compared to the corresponding control (UP Hsp60 U). On the other hand, both antimycin A only and AA + UP resulted in up-regulated TNF-α expression. Surprisingly, TNF-α expressions in antimycin A only conditions were very low, that the bands for 5 (TNF-α 5) and 25 μM (TNF-α 25) were hardly visible. This did not happen when uridine and pyruvate were added. The particular up-regulated TNF-α expression in 50μM antimycin A plus UP could also be an outlier. For all three genes of interest, PCR products from 10 and

50 μM of antimycin A only did not show up as the RNA was immediately degraded after extraction in 10 μM, which was seen as a smear at the lower part of the formaldehyde gel (Figure 11), and the RNA yield for 50 μM was too low (Table 18).

Table 19: Band areas of PCR products were quantified and normalised against GAPDH expressions using Gel Quant software (table continued through page 73 to 75).

GAPDH or GAP = human GAPDH gene; Hsp60 = human Hsp60 gene; TNF-α = human TNF-α gene. U = untreated control; UP = uridine and pyruvate were added; 5, 10, 25, 50 = respective antimycin A concentrations in μM. Band areas for 10 and 50 μM antimycin A only were missing because a) RNA from 10 μM antimycin A treatment was degraded immediately after extraction and b) the RNA yield from 50 μM antimycin A treatment was too low to produce PCR products.

Gene, AA Conc	Area	gene/GAPDH
GAPDH 5	159718	1
GAPDH 10	0	0
GAPDH 25	96046	1
GAPDH 50	0	0
GAPDH U	147815	1
UP GAP 5	164737	1
UP GAP 10	149606	1
UP GAP 25	140249	1
UP GAP 50	154547	1
UP GAP U	151802	1

Gene, AA Conc	Area	gene/GAPDH
Hsp60 5	101957	0.6384
Hsp60 10	0	0
Hsp60 25	41362	0.4306
Hsp60 50	0	0
Hsp60 U	107043	0.7242
UP Hsp60 5	113140	0.6868
UP Hsp60 10	118726	0.7936
UP Hsp60 25	138456	0.9872
UP Hsp60 50	133055	0.8609
UP Hsp60 U	139472	0.9188
TNF-α 5	4522	0.0283
TNF-α 10	0	0
TNF-α 25	7834	0.0816
TNF-α 50	0	0
TNF-α U	70972	0.4801
UP TNF-α 5	77390	0.4698

Gene, AA Conc	Area	gene/GAPDH
UP TNF-α 10	41414	0.2768
UP TNF-α 25	77433	0.5521
UP TNF-α 50	111719	0.7229
UP TNF-α U	77232	0.5088

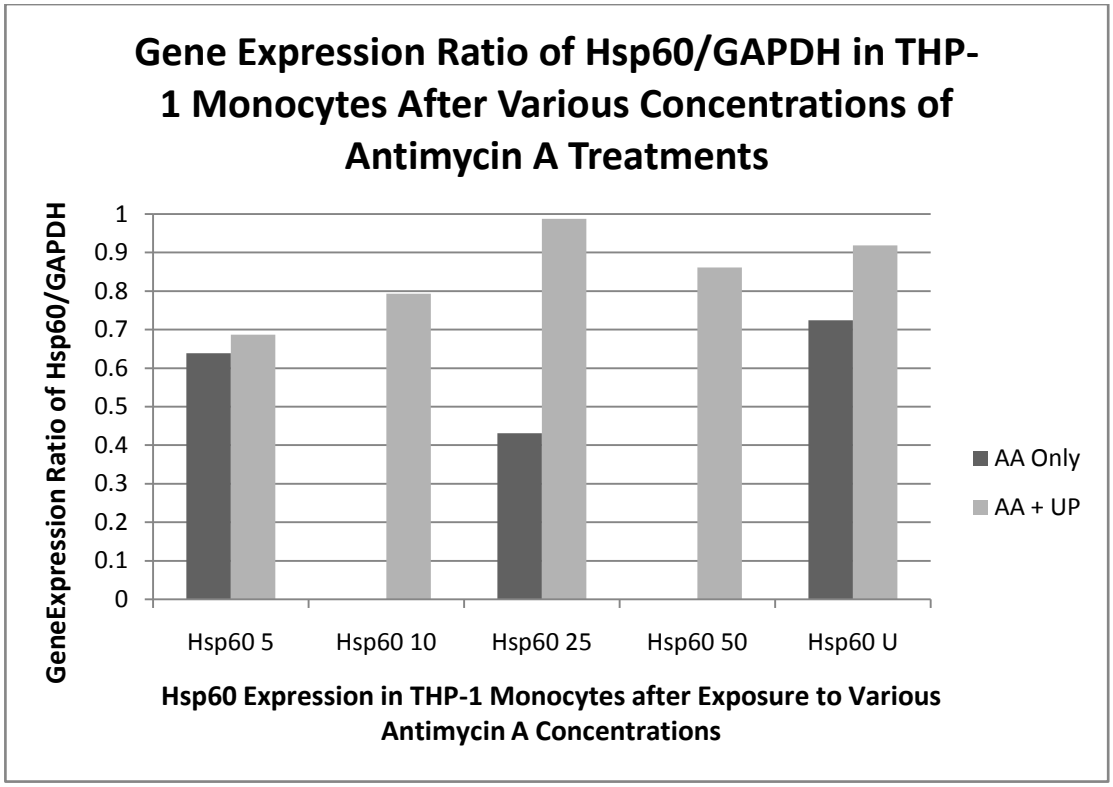

Figure 16: Gene expression of human Hsp60 normalised with human GAPDH in THP-1 monocytes, after various concentrations of antimycin A challenge (5, 10, 25 and 50 µM), with or without 50 µg/mL uridine and 1 mM sodium pyruvate (n = 1).

U = untreated control; UP = uridine and pyruvate were added.

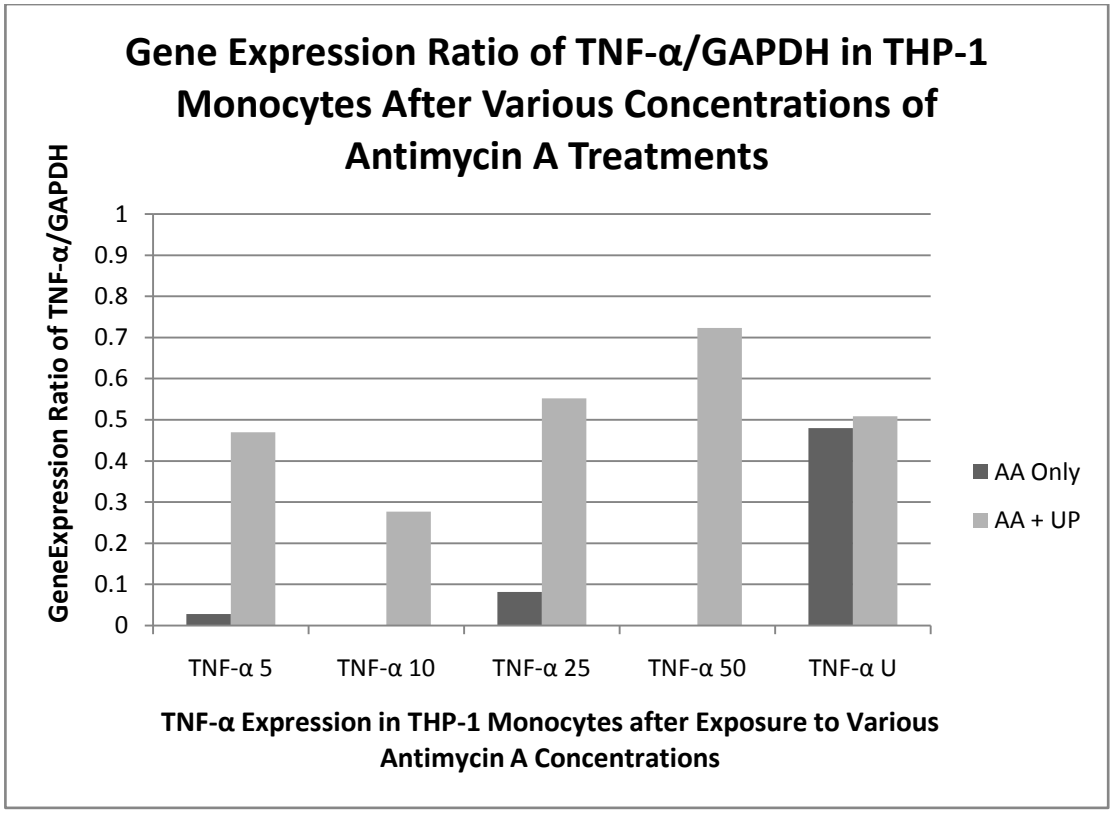

Figure 17: Gene expression of human TNF-α normalised with human GAPDH in THP-1 monocytes, after various concentrations of antimycin A challenge (5, 10, 25 and 50 µM), with or without 50 µg/mL uridine and 1 mM sodium pyruvate (n = 1).

U = untreated control; UP = uridine and pyruvate were added.

CHAPTER SIX DISCUSSION

6.1 Antimycin A Dose-Response Assays with THP-1 Monocytes

The antimycin A inhibition on THP-1 cells was dose-dependent. The conditioned media after antimycin A treatment was yellower than the controls. Since cells with compromised mitochondrial activities convert pyruvate to lactate in order to generate NAD^+, and the yellow media indicates increased acidity, we interpreted that there were some mitochondrial stress or damage in THP-1 monocytes. Ethanol, as the solvent for antimycin A, did not significantly change the growth rate of THP-1 monocytes relative to the untreated controls, either (Table 13). Interestingly, the application of uridine and pyruvate did not significantly increase THP-1 cell growth under the exposure of antimycin A. This could be due to the high concentration of antimycin A used that over-rode the redox rescue effect, as only 5−25 nM antimycin A were added to HL60 cells (Mills *et al*., 1999). It is therefore worth treating THP-1 monocytes with lower antimycin A concentrations in the future to test the functioning of redox rescuing compounds.

From this series of experiments we know how many live cells there were on each day. However we did not measure the activity of mitochondrial complexes, so we do not

know exactly how much mitochondrial stress/inhibition there was with various antimycin A concentrations. Besides, MAPK/ERKs activated by hydrogen peroxide-mediated oxidative stress model was found to be ATP- and mitochondrion-dependent in H9c2 cells (Abas *et al*., 2000). Because Hsp60 was found to activate NF-κB through similar signal cascade, the activities of such signal pathway could also be assessed while antimycin A or other mitochondrial inhibitors are used in the future.

Triplicates are only the minimal sample size for statistical analysis. The replications for each antimycin A concentration of dose-response assays could be increased to obtain better statistical analyses. The exposure time of antimycin A to THP-1 monocytes could be increased to monitor the long-term effect of mitochondrial stress.

6.2 TRIzol RNA Extraction

Total RNA from THP-1 monocytes after five days of exposure to various antimycin A concentrations were extracted using TRIzol and chloroform. Solvent controls were eliminated as they were shown not to significantly change THP-1 cell growth compared to the untreated controls (Table 13). The mRNA of human GAPDH, Hsp60 and TNF-α expressed by THP-1 monocytes after the five-day dose-response assay were determined by RT-PCR.

TRIzol (Invitrogen) -chloroform successfully extracted total RNA out of THP-1 monocytes when the cell concentration was at least 10^5 cells/mL. The centrifuging speed for making cell pellet was crucial for good purity and amount of RNA extracted. If too low, not enough cells could be retained to extract RNA. If the speed was too high, the cells would be lysed thus losing RNA into supernatant, as well as degradation occurring via released RNases. The crude RNA still contained some DNA residues because the product was not filtered through a column like some RNA extraction kits do. The purity and amount were therefore more dependent on an operator's skill. The reason for a complete degradation of RNA straight after extraction (Figure 11) remains to be discovered.

6.3 RT-PCR

It is well-known that stress proteins such as Hsp60 can be up-regulated during cellular and/or mitochondrial stress (Martinus *et al*., 1996), and Hsp60 can be cyto-protective and anti-apoptotic (Kirchhoff *et al*., 2002). We checked to see if THP-1 cells treated with antimycin A had higher levels of Hsp60 expression at the mRNA level. Since THP-1 is also a monocytic cell line, we decided to also see if inhibiting mitochondrial function via antimycin A has any effects on the ability of cells to modulate TNF-α expression.

The RT-PCR functioned correctly. No detectable contaminations showed up according to the negative controls (Figure 14 and -15). Total RNA extracted from THP-1 monocytes, after antimycin A dose-response assays were used to run RT-PCR. We know the extent of human GAPDH, Hsp60 and TNF-α mRNA level after five days of antimycin A exposure by viewing the results from non-reducing agarose gel electrophoresis. The band areas on the agarose gel were quantified using Gel Quant software. The amount of Hsp60 and TNF-α mRNA was compared against GAPDH and expressed as ratios of Hsp60 band area/corresponding GAPDH band area or TNF-α band area/corresponding GAPDH band area (Table 19).

Yet we do not know the amount of GAPDH, Hsp60 and TNF-α mRNA produced during the previous four days of antimycin A dose-response assay. Quantitative real-time PCR could be done in the future to closely monitor the gene expression of THP-1 monocytes undergoing mitochondrial stress/dysfunction.

The Hsp60 gene expression level, as seen by mRNA in Figure 16, decreased with increasing antimycin A concentration when no uridine and pyruvate (UP) were added to THP-1 monocytes, but Hsp60 was up-regulated as antimycin A concentration raised in the presence of UP. It could be that the up-regulated Hsp60 in UP-treated THP-1 monocytes was to respond to the enhanced mitochondrial stress as the antimycin A concentration increased. However this does not explain why down-

regulation of Hsp60 was seen in THP-1 monocytes treated with antimycin A only. Or else the increased Hsp60 mRNA in UP-treated monocytes could simply be due to higher cell density, since some up-regulation of Hsp60 was seen in the UP untreated control. Moreover, Hsp60 is also seen as a danger signal in the immune system and has inflammatory induction effects. It has been shown that adding recombinant human Hsp60 to THP-1-derived macrophages can induce them to produce TNF-α at a level comparable to bacterial Hsp60 (Ueki *et al*., 2002); and monocytes are known to detect one's own Hsp60 through cell surface receptors such as TLR4 to activate NF-κB then produce TNF-α (Yang *et al*., 2008). The role(s) of Hsp60 in monocytes with compromised mitochondrial functions thus need to be further investigated.

The TNF-α expression in THP-1 monocytes exposed to only antimycin A was down-regulated relative to the untreated control that the bands were hardly visible on the agarose gel (Figure 17). This kind of dramatic down-regulation of TNF-α was not detected in the corresponding antimycin A concentrations together with uridine and pyruvate. Uridine and/or pyruvate may have other functions in cells apart from redox rescue and pyrimidine biosynthesis fulfilment. The reason for such expression difference also remains to be determined as no literatures at this stage could be found to explain so.

Although both Hsp60 and TNF-α expressions were up-regulated in THP-1 monocytes treated with antimycin A, uridine and pyruvate (UP), there appears to be minor differences in the expression of these two genes. The expression of Hsp60 mostly did not exceed the UP untreated control, even though elevated (Figure 16). Nevertheless, TNF-α expressions were mainly more strongly or equal to the UP untreated control (Figure 17). Investigating the reason underlying could also be another future direction.

The major short fall of this series of RT-PCR work is that no repetitions were done (n = 1). This means no statistical analyses could be carried out to normalise operational and systematic errors. Such errors can be amplified if the expression levels are very low, as in the case of TNF-α. Moreover, errors can occur while manually selecting band areas to analyse with Gel Quant. More replications of the whole set of experiment, from does-response assay to RT-PCR, along with appropriate statistical analyses should be done before drawing any conclusions. Additionally, GAPDH, Hsp60 and TNF-α expression may be checked at the protein level via Western Blot and enzyme-linked immunosorbent assay (ELISA) to confirm their up- or down-regulations. These could also be the future work of this project.

REFERENCES

Abas, L., Bogoyevitch, M. A. & Guppy, M. 2000. Mitochondrial ATP production is necessary for activation of the extracellular-signal-regulated kinases during ischaemia/reperfusion in rat myocyte-derived H9c2 cells. *Biochemical Journal*, 349, 119-126.

Alcain, F. J., Buron, M. I., Villalba, J. M. & Navas, P. 1991. Ascorbate is regenerated by HL-60 cells through the transplasmalemma redox system. *Biochimica et Biophysica Acta*, 1073, 380-385.

Arsenijevic, D., Onuma, H., Pecqueur, C., Raimbault, S., Manning, B. S., Miroux, B., Couplan, E., Alves-Guerra, M. C., Goubern, M., Surwit, R., Bouillaud, F., Richard, D., Collins, S. & Ricquier, D. 2000. Disruption of the uncoupling protein-2 gene in mice reveals a role in immunity and reactive oxygen species production. *Nature Genetics*, 26, 435-439.

Auwerx, J. 1991. The human leukemia cell line, THP-1: a multifacetted model for the study of monocyte-macrophage differentiation. *Experientia*, 47, 22-31.

Bailey, S. M., Landar, A. & Darley-Usmar, V. 2005. Mitochondrial proteomics in free radical research. *Free Radical Biology and Medicine*, 38, 175-188.

Bozner, P., Wilson, G. L., Druzhyna, N. M., Bryant-Thomas, T. K., LeDoux, S. P., Wilson, G. L. & Pappolla, M. A. 2002. Deficiency of chaperonin 60 in Down's syndrome. *Journal of Alzheimer's Disease*, 4, 479 - 486

Centonze, D., Finazzi-Agro, A., Bernardi, G. & Maccarrone, M. 2007. The endocannabinoid system in targeting inflammatory neurodegenerative diseases. *Trends in Pharmacological Sciences*, 28, 180-187.

Chen, W., Syldath, U., Bellmann, K., Burkart, V. & Kolb, H. 1999. Human 60-kDa Heat-Shock Protein: A Danger Signal to the Innate Immune System. *J Immunol*, 162, 3212-3219.

del Castillo-Olivares, A., de Castro, I. N. & Medina, M. A. 2000. Dual role of plasma membrane electron transport systems in defense. *Critical Reviews in Biochemistry and Molecular Biology*, 35, 197-220.

Droge, W. 2002. Free Radicals in the Physiological Control of Cell Function. *Physiol. Rev.*, 82, 47-95.

Elias, D., Reshef, T., Birk, O. S., van der Zee, R., Walker, M. D. & Cohen, I. R. 1991. Vaccination Against Autoimmune Mouse Diabetes with a T-Cell Epitope of the Human 65-kDa Heat Shock Protein. *Proceedings of the National Academy of Sciences*, 88, 3088-3091.

Esiri, M. M. 2007. The interplay between inflammation and neurodegeneration in CNS disease. *Journal of Neuroimmunology*, 184, 4-16.

Firth, A. L., Yuill, K. H. & Smirnov, S. V. 2008. Mitochondria-dependent regulation of Kv currents in rat pulmonary artery smooth muscle cells. *American Journal of Physiology-Lung Cellular and Molecular Physiology*, 295, L61-L70.

Fleury, C., Mignotte, B. & Vayssiere, J. L. 2002. Mitochondrial reactive oxygen species in cell death signaling. *Biochimie*, 84, 131-141.

Garret, R. H. & Grisham, C. M. 2005. Biochemistry. In: *Biochemistry*. Belmont: Thomson Brooks/Cole.

Giardina, T. M., Steer, J. H., Lo, S. Z. Y. & Joyce, D. A. 2008. Uncoupling protein-2 accumulates rapidly in the inner mitochondrial membrane during mitochondrial reactive oxygen stress in macrophages. *Biochimica Et Biophysica Acta-Bioenergetics*, 1777, 118-129.

Gómez-Díaz, C., Villalba, J. M., Pérez-Vicente, R., Crane, F. L. & Navas, P. 1997. Ascorbate Stabilization Is Stimulated in [rho]°HL-60 Cells by CoQ10Increase at the Plasma Membrane. *Biochemical and Biophysical Research Communications*, 234, 79-81.

Guidarelli, A., Sciorati, C., Clementi, E. & Cantoni, O. 2006. Peroxynitrite mobilizes calcium ions from ryanodine-sensitive stores, a process associated with the mitochondrial accumulation of the cation and the enforced formation of species mediating cleavage of genomic DNA. *Free Radical Biology and Medicine*, 41, 154-164.

Gupta, R. S. & Austin, R. C. 1987. Mitochondrial Matrix Localization of a Protein Altered in Mutants Resistant to the Microtubule Inhibitor Podophyllotoxin. *Eur J Cell Bio*, 45, 170-176.

Gupta, S. & Knowlton, A. A. 2007. HSP60 trafficking in adult cardiac myocytes: role of the exosomal pathway. *American Journal of Physiology-Heart and Circulatory Physiology*, 292, H3052-H3056.

Halliwell, B. 1992. Reactive oxygen species and the central-nervous-system. *Journal of Neurochemistry*, 59, 1609-1623.

Halliwell, B. 2001. Role of free radicals in the neurodegenerative diseases - Therapeutic implications for antioxidant treatment. *Drugs & Aging*, 18, 685-716.

Hartl, F. U. 1996. Molecular chaperones in cellular protein folding. *Nature*, 381, 571-580.

Huang, L.-s., Cobessi, D., Tung, E. Y. & Berry, E. A. 2005. Binding of the Respiratory Chain Inhibitor Antimycin to the Mitochondrial bc1 Complex: A New Crystal Structure Reveals an Altered Intramolecular Hydrogen-bonding Pattern. *Journal of Molecular Biology*, 351, 573-597.

Hyun, D. H., Hunt, N. D., Emerson, S. S., Hernandez, J. O., Mattson, M. P. & de Cabo, R. 2007. Up-regulation of plasma membrane-associated redox activities in neuronal cells lacking functional mitochondria. *Journal of Neurochemistry*, 100, 1364-1374.

Jones, M. E. 1980. Pyrimidine Nucleotide Biosynthesis in Animals: Genes, Enzymers, and Regulation of UMP Biosynthesis. *Annual Reviews of Biochemistry*, 49, 253-279.

Kagan, V. E., Serbinova, E. A. & Packer, L. 1990a. Generation and recycling of radicals from phenolic antioxidants. *Archives of Biochemistry and Biophysics*, 280, 33-39.

Kagan, V. E., Serbinova, E. A. & Packer, L. 1990b. Recycling and antioxidant activity of tocopherol homologs of differing hydrocarbon chain lengths in liver-microsomes. *Archives of Biochemistry and Biophysics*, 282, 221-225.

King, M. & Attardi, G. 1989. Human Cells Lacking mtDNA: Repopulation with Exogenous Mitochondria by Complementation. *Science*, 246, 500-503.

Kirchhoff, S. R., Gupta, S. & Knowlton, A. A. 2002. Cytosolic heat shock protein 60, apoptosis, and myocardial injury. *Circulation*, 105, 2899-2904.

Klann, E., Roberson, E. D., Knapp, L. T. & Sweatt, J. D. 1998. A role for superoxide in protein kinase C activation and induction of long-term potentiation. *Journal of Biological Chemistry*, 273, 4516-4522.

Lancaster, G. I. & Febbraio, M. A. 2005. Exosome-dependent Trafficking of HSP70: A NOVEL SECRETORY PATHWAY FOR CELLULAR STRESS PROTEINS. *J. Biol. Chem.*, 280, 23349-23355.

Larm, J. A., Vaillant, F., Linnane, A. W. & Lawen, A. 1994. Up-regulation of the plasma-membrane oxidoreductase as a prerequisite for the viability of human Namalwa RHO(0) cells. *Journal of Biological Chemistry*, 269, 30097-30100.

Lewthwaite, J. C., Clarkin, C. E., Coates, A. R. M., Poole, S., Lawrence, R. A., Wheeler-Jones, C. P. D., Pitsillides, A. A., Singh, M. & Henderson, B. 2007.

Highly homologous Mycobacterium tuberculosis chaperonin 60 proteins with differential CD14 dependencies stimulate cytokine production by human monocytes through cooperative activation of p38 and ERK1/2 mitogen-activated protein kinases. *International Immunopharmacology*, 7, 230-240.

Lin, K. M., Lin, B., Lian, I. Y., Mestril, R., Scheffler, I. E. & Dillmann, W. H. 2001. Combined and individual mitochondrial HSP60 and HSP10 expression in cardiac myocytes protects mitochondrial function and prevents apoptotic cell deaths induced by simulated ischemia-reoxygenation. *Circulation*, 103, 1787-1792.

Maguire, M., Coates, A. R. M. & Henderson, B. 2002a. Chaperonin 60 unfolds its secrets of cellular communication. *Cell Stress Chaperones*, 7, 317–329.

Maguire, M., Coates, A. R. M. & Henderson, B. 2002b. Chaperonin 60 unfolds its secrets of cellular communication. *Cell Stress & Chaperones*, 7, 317-329.

Mak, T. W. & Saunders, M. E. 2006. *The Immune Response*: Elsevier Inc.

Martinus, R. D., Garth, G. P., Webster, T. L., Cartwright, P., Naylor, D. J., Hoj, P. B. & Hoogenraad, N. J. 1996. Selective induction of mitochondrial chaperones in response to loss of the mitochondrial genome. *European Journal of Biochemistry*, 240, 98-103.

Martinus, R. D., Linnane, A. W. & Nagley, P. 1993. Growth of RHO(0) human Namalwa cells lacking oxidative-phosphorylation can be sustained by redox compounds potassium ferricyanide or coenzyme q(10) putatively acting through the plasma-membrane oxidase. *Biochemistry and Molecular Biology International*, 31, 997-1005.

Mattson, M. P. & Kroemer, G. 2003. Mitochondria in cell death: novel targets for neuroprotection and cardioprotection. *Trends in Molecular Medicine*, 9, 196-205.

McCord, J. M. 2000. The evolution of free radicals and oxidative stress. *American Journal of Medicine*, 108, 652-659.

Mills, K. I., Woodgate, L. J., Gilkes, A. F., Walsh, V., Sweeney, M. C., Brown, G. & Burnett, A. K. 1999. Inhibition of mitochondrial function in HL60 cells is associated with an increased apoptosis and expression of CD14. *Biochemical and Biophysical Research Communications*, 263, 294-300.

Morais, R., Gregoire, M., Jeanotte, L. & Gravel, D. 1980. Chick Embryo Cells Rendered Respiratory-Deficient by Chloramphenicol and Ethidium Bromide are Auxothrophic for Pyrimidines. *Biochemical and Biophysical Research Communications*, 94, 71-77.

Nagley, P., Sriprakash, K. S. & Linnane, A. W. 1977. In: *Advances in Microbial Physiology* (Ed. by Rose, A. H. & Tempest, D. W.), pp. 157-277. London: Acedamic Press.

Nohl, H., Gille, L., Kozlov, A. & Staniek, K. 2003. Are mitochondria a spontaneous and permanent source of reactive oxygen species? *Redox Report*, 8, 135-141.

Omar, B. A. & McCord, J. M. 1991. Interstitial equilibration of superoxide-dismutase correlates with its protective effect in the isolated rabbit heart. *Journal of Molecular and Cellular Cardiology*, 23, 149-159.

Piskemik, C., Haindl, S., Behling, T., Gerald, Z., Kehrer, I., Redl, H. & Kozlov, A. V. 2008. Antimycin A and lipopolysaccharide cause the leakage of superoxide radicals from rat liver mitochondria. *Biochimica Et Biophysica Acta-Molecular Basis of Disease*, 1782, 280-285.

Pockley, A. G. 2003. Heat shock proteins as regulators of the immune response. *Lancet*, 362, 469-476.

Praeres da Costa, C. U. I., Wagner, H. & Miethke, T. C. 2003. Heat shock protein-mediated activation of innate immune cells. In: *Heat shock protein and inflammation* (Ed. by van Eden, W.), pp. 43-54. Basel, Switzerland: Birkhauser Verlag.

Randord, J., Coates, A. & Henderson, B. 2000. Chaperonins are cell-signalling proteins: The Unfolding Biology of Molecular Chaperones. *Expert Reviews*, 15.

Reddy, P. H. & Beal, M. F. 2005. Are mitochondria critical in the pathogenesis of Alzheimer's disease? *Brain Research Reviews*, 49, 618-632.

Reed, J., Reed, T. A. & Hess, B. 1978. Circular-Dichroism Studies of the Cytochrome *b*-c_1 Complex of *Saccharomyces cerevisiae*. *European Journal of Biochemistry*, 91, 255-261.

Ritossa, F. A. 1962. A New Puffing Pattern Induced by Temperature Shock and DNP in Drosophilia. *Experientia*, 18, 571-573.

Sambrook, J., Fritsch, E. F. & Maniatis, T. 1989. Extraction, Purification, and Analysis of Messenger RNA from Eukaryotic Cells. In: *Molecular Cloning - A*

Laboratory Manual (Ed. by Nolan, C.), pp. 7.3-7.84. New York: Cold Spring Harbor Laboratory Press.

Sastre, J., Pallardo, F. V. & Vina, J. 2003. The role of mitochondrial oxidative stress in aging. *Free Radical Biology and Medicine*, 35, 1-8.

Schwartz, M. & Cohen, I. R. 2000. Autoimmunity can benefit self-maintenance. *Immunology Today*, 21, 265-268.

Slater, E. C. 1973. The Mechanism of Action of the Respiratory Inhibitor, Antimycin. *Biochimica et Biophysica Acta*, 301, 129-154.

Thompson, B. Y., Sivam, G., Britigan, B. E., Rosen, G. M. & Cohen, M. S. 1988. Oxygen Metabolism of the HL-60 Cell Line: Comparison of the Effects of Monocytoid and Neutrophilic Differentiation. *Journal of Leukocyte Biology*, 43, 140-147.

Tissieres, A., Mitchell, H. K. & Tracey, U. 1974. Protein Synthesis in Salivary Glands of *Drosophila melanogaster*: Relation to Chromosome Puffs. *Journal of Molecular Biology*, 84, 389-398.

Tse, H. M., Milton, M. J. & Piganelli, J. D. 2004. Mechanistic analysis of the immunomodulatory effects of a catalytic antioxidant on antigen-presenting cells: Implication for their use in targeting oxidation-reduction reactions in innate immunity. *Free Radical Biology and Medicine*, 36, 233-247.

Tytell, M. & Hooper, P. L. 2001. Heat shock proteins: new keys to the development of cytoprotective therapies. *Expert Opin Ther Targets.*, 5, 267-287.

Ueki, K., Tabeta, K., Yoshie, H. & Yamazaki, K. 2002. Self-heat shock protein 60 induces tumour necrosis factor-alpha in monocyte-derived macrophage: possible role in chronic inflammatory periodontal disease. *Clinical and Experimental Immunology*, 127, 72-77.

Vaillant, F., Loveland, B. E., Nagley, P. & Linnane, A. W. 1991. Some biochemical-properties of human lymphoblastoid Namalwa cells grown anaerobically. *Biochemistry International*, 23, 571-580.

Vaille, A., Jadot, G. & Elizagaray, A. 1990. Anti-inflammatory activity of various superoxide dismutases on polyarthritis in the Lewis rat. *Biochemical Pharmacology*, 39, 247-255.

Veereshwarayya, V., Kumar, P., Rosen, K. M., Mestril, R. & Querfurth, H. W. 2006. Differential effects of mitochondrial heat shock protein 60 and related molecular chaperones to prevent intracellular beta-amyloid-induced inhibition of complex IV and limit apoptosis. *Journal of Biological Chemistry*, 281, 29468-29478.

Wallin, R. P. A., Lundqvist, A., More, S. H., von Bonin, A., Kiessling, R. & Ljunggren, H.-G. 2002. Heat-shock proteins as activators of the innate immune system. *Trends in Immunology*, 23, 130-135.

Wikowski, J. & Zoller, M. 2001. Polymerase Chain Reaction. In: *Recombinant DNA* (Ed. by Watson, J. D. & Gilman, M.), pp. 79-98. New York: W.H. Freeman and Company.

Yang, Q. W., Li, J. C., Lu, F. L., Wen, A. Q., Xiang, J., Zhang, L. L., Huang, Z. Y. & Wang, J. Z. 2008. Upregulated expression of toll-like receptor 4 in monocytes

correlates with severity of acute cerebral infarction. *Journal of Cerebral Blood Flow and Metabolism*, 28, 1588-1596.

Zanin-Zhorov, A., Bruck, R., Tal, G., Oren, S., Aeed, H., Hershkoviz, R., Cohen, I. R. & Lider, O. 2005. Heat Shock Protein 60 Inhibits Th1-Mediated Hepatitis Model via Innate Regulation of Th1/Th2 Transcription Factors and Cytokines. *J Immunol*, 174, 3227-3236.

Zhao, Y., Yokota, K., Ayada, K., Yamamoto, Y., Okada, T., Shen, L. & Oguma, K. 2007. Helicobacter pylori heat-shock protein 60 induces interleukin-8 via a Toll-like receptor (TLR)2 and mitogen-activated protein (MAP) kinase pathway in human monocytes. *J Med Microbiol*, 56, 154-164.

Zhuang, J. G., Ren, Y., Snowden, R. T., Zhu, H. J., Gogvadze, V., Savill, J. S. & Cohen, G. M. 1998. Dissociation of phagocyte recognition of cells undergoing apoptosis from other features of the apoptotic program. *Journal of Biological Chemistry*, 273, 15628-15632.